

# 1 The case for a New Frontiers-class Uranus Orbiter: System science at an 2 underexplored and unique world with a mid-scale mission

5 Ian J. Cohen<sup>1,2</sup>, Chloe Beddingfield<sup>3,4</sup>, Robert Chancia<sup>5,6</sup>, Gina DiBraccio<sup>7</sup>,  
6 Matthew Hedman<sup>5</sup>, Shannon MacKenzie<sup>2</sup>, Barry Mauk<sup>2</sup>, Kunio M. Sayanagi<sup>8</sup>, Krista M.  
7 Soderlund<sup>9</sup>, Elizabeth Turtle<sup>2</sup>, Caitlin Ahrens<sup>5</sup>, Christopher S. Arridge<sup>10</sup>, Shawn  
8 M. Brooks<sup>11</sup>, Emma Bunce<sup>12</sup>, Sebastien Charnoz<sup>13</sup>, Athena Coustenis<sup>14</sup>, Robert A.  
9 Dillman<sup>15</sup>, Soumyo Dutta<sup>13</sup>, Leigh N. Fletcher<sup>10</sup>, Rebecca Harbison<sup>16</sup>, Ravit  
10 Helled<sup>17</sup>, Richard Holme<sup>18</sup>, Lauren Jozwiak<sup>2</sup>, Yasumasa Kasaba<sup>19</sup>, Peter Kollmann<sup>2</sup>,  
11 Statia Luszcz-Cook<sup>20,21</sup>, Kathleen Mandt<sup>2</sup>, Olivier Mousis<sup>22</sup>, Alessandro Mura<sup>23</sup>, Go  
12 Murakami<sup>24</sup>, Marzia Parisi<sup>9</sup>, Abigail Rymer<sup>2</sup>, Sabine Stanley<sup>25</sup>, Katrin Stephan<sup>26</sup>,  
13 Ronald J. Vervack, Jr.<sup>2</sup>, Michael H. Wong<sup>27</sup>, and Peter Wurz<sup>28</sup>

<sup>1</sup> Corresponding author Ian.Cohen@jhuapl.edu

<sup>2</sup> The Johns Hopkins Applied Physics Laboratory, Space Exploration Sector, Laurel, MD 20723, USA

<sup>3</sup> The SETI Institute, Mountain View, CA 94043, USA

<sup>4</sup> NASA Ames Research Center, Space Science and Astrobiology Division, Mountain View, CA 94043, USA

<sup>5</sup> University of Idaho, Department of Physics, Moscow, ID 83844, USA

<sup>6</sup> now at Rochester Institute of Technology, Chester F. Carlson Center for Imaging Science, Rochester, NY 14623, USA

<sup>7</sup> NASA Goddard Space Flight Center, Sciences and Exploration Directorate, Greenbelt, MD 20771, USA

<sup>8</sup> Hampton University, Department of Atmospheric and Planetary Sciences, Hampton, VA 23668, USA

<sup>9</sup> University of Texas at Austin, Institute for Geophysics, Austin, TX 78758, USA

<sup>10</sup> University of Lancaster, Department of Physics, Lancaster, LA1 4YW, United Kingdom

<sup>11</sup> Jet Propulsion Laboratory, California Institute of Technology, Pasadena, CA 91109, USA

<sup>12</sup> University of Leicester, School of Physics and Astronomy, Leicester, LE1 7RH, United Kingdom  
<sup>13</sup> University of Paris/Paris Globe Institute of Physics, Department of Cosmochemistry, Astrophysics and

<sup>14</sup> Center National de la Recherche Scientifique (CNRS)/Laboratoire d'Etudes Spatiales et d'Instrumentation en

Astrophysique (LESIA)/Paris-Meudon Observatory, 92190 Meudon, France

<sup>15</sup> NASA Langley Research Center, Hampton, VA 23666, USA

<sup>16</sup> University of Nebraska-Lincoln, Department of Physics & Astronomy, Lincoln, NE 68588, USA  
<sup>17</sup> University of Zurich, Center for Theoretical Astrophysics & Cosmology, Institute for Computational Science, 190

CH-8057 Zurich, Switzerland

<sup>18</sup> University of Liverpool, Department of Earth, Ocean and Ecological Sciences, Liverpool, L69 3BX, United Kingdom.

**Kingdom**  $\frac{10}{10} = \frac{10}{10}$  **Health**  $\frac{10}{10} = \frac{10}{10}$  **Energy**  $\frac{10}{10} = \frac{10}{10}$  **Food**  $\frac{10}{10} = \frac{10}{10}$  **Water**  $\frac{10}{10} = \frac{10}{10}$  **Shelter**  $\frac{10}{10} = \frac{10}{10}$  **Sanitation**  $\frac{10}{10} = \frac{10}{10}$

<sup>19</sup> Tohoku University, Planetary Plasma and Atmospheric Research Center, Aoba, Sendai, Japan.

<sup>20</sup> American Museum of Natural History, Department of Astrophysics, New York, NY 10024, U.S.A.  
<sup>21</sup> Cf. G. H. Hubble, *Proc. Natl. Acad. Sci.*, **31**, 424 (1945).

<sup>21</sup> Columbia University, Department of Astronomy, New York, New York 10027, USA  
<sup>22</sup> Aix Marseille Université, Laboratoire d’Astrophysique de Marseille, 13013 Marseille, France  
<sup>23</sup> Institut National de la Science de l’Univers (IN2P3), CNRS, Université Grenoble Alpes, 38054 Grenoble Cedex 9, France

<sup>23</sup> Istituto Nazionale di Astrofisica (INAF)/Istituto di Astrofisica e Planetologia Spaziali (IAPS), 00133, Roma, Rome, Italy

<sup>24</sup> Institute of Space and Astronautical Science, Japan Aerospace Exploration Agency, Sagamihara, Kanagawa 5210, Japan

<sup>25</sup> Johns Hopkins University, Morton K. Blaustein Department of Earth & Planetary Sciences, Baltimore, MD 21218, USA

<sup>26</sup> German Aerospace Center (DLR), Institute of Planetary Research, Rutherfordstrasse 2, 12489 Berlin, Germany  
<sup>27</sup> University of California, Berkeley, Department of Earth and Planetary Sciences, Berkeley, CA 94720, USA

<sup>27</sup> University of California, Berkeley, Department of Astronomy, Berkeley, CA 94720, USA

<sup>28</sup> University of Bern, Space Exploration and Planetary Division, Hochschulstrasse 6, 3012 Bern, Switzerland

14

## Abstract

15 Current knowledge of the Uranian system is limited to observations from the  
16 flyby of Voyager 2 and limited remote observations. However, Uranus remains a  
17 highly compelling scientific target due to the unique properties of many  
18 aspects of the planet itself and its system. Future exploration of Uranus  
19 must focus on cross-disciplinary science that spans the range of research  
20 areas from the planet's interior, atmosphere, and magnetosphere to the its  
21 rings and satellites, as well as the interactions between them. Detailed  
22 study of Uranus by an orbiter is crucial not only for valuable insights into  
23 the formation and evolution of our solar system but also for providing ground  
24 truths for the understanding of exoplanets. As such, exploration of Uranus  
25 will not only enhance our understanding of the Ice Giant planets themselves  
26 but also extends to planetary dynamics throughout our solar system and  
27 beyond. The timeliness of exploring Uranus is great as the community hopes to  
28 return in time to image unseen portions of the satellites and magnetospheric  
29 configurations. This urgency motivates evaluation of what science can be  
30 achieved with a lower-cost, potentially faster-turnaround mission, such as a  
31 New Frontiers (NF)-class orbiter mission. This paper outlines the scientific  
32 case for and the technological and design considerations that must be  
33 addressed by future studies to enable a NF-class Uranus orbiter with balanced  
34 cross-disciplinary science objectives. In particular, studies that trade  
35 scientific scope and instrumentation and operational capabilities against  
36 simpler and cheaper options must be fundamental to the mission formulation.

37

38 1 Introduction

39     Uranus presents a compelling scientific target, providing a unique  
40 opportunity to explore an Ice Giant system with its five classical satellites,  
41 potential ocean worlds with drastic surface features, and dynamically full and  
42 apparently haphazard system of rings and small moons, in addition to the  
43 planetary and magnetospheric effects of its highly-tilted rotational axis being  
44 almost in Uranus' orbit plane and its strongly multipolar intrinsic magnetic  
45 field. Uranus, and its Ice Giant neighbor Neptune, represents a distinct class  
46 of planets in the solar system and beyond. Whereas Jupiter and Saturn are made  
47 mostly of hydrogen, the bulk compositions of Uranus and Neptune are dominated  
48 by heavier "ices" such as water, methane, hydrogen sulfide, and ammonia. These  
49 "Ice Giants" may be representative of similarly-sized planets common throughout  
50 the galaxy (Batalha et al. 2011; Wakeford & Dalba 2020), but remain the least-  
51 investigated planets in the solar system. The observations from Voyager 2 have  
52 left us with many outstanding mysteries about the Uranian system (e.g., Fletcher  
53 et al. 2020a; 2020c). As such, the study of the solar system's Ice Giants is a  
54 crucial step for providing ground truths for the understanding of Ice Giant-  
55 sized exoplanets (Rymer et al. 2018; Fortney et al. 2021; Wakeford & Dalba 2021)  
56 as observations show that Neptune-sized planets are the most abundant population  
57 of exoplanets (Zhu & Dong 2021).

58     The 2011 National Research Council Planetary Science Decadal Survey *Vision*  
59 and *Voyages for Planetary Science in the Decade 2013-2022* states: "The ice  
60 giants are thus one of the great remaining unknowns in the solar system, the  
61 only class of planet that has never been explored in detail" (National Research  
62 Council 2011). Underscoring the importance of studying the Ice Giants, the 2013  
63 Decadal Survey recommended a Uranus Orbiter and Probe as the third-highest  
64 priority "large-class" mission (National Research Council 2011). The mission  
65 summarized here would explicitly address the design considerations necessary to  
66 formulate an orbiter mission to Uranus within a future New Frontiers cost cap  
67 (assumed to be approximately \$1B USD). A recommendation for a similar mission  
68 concept was submitted by the Outer Planets Assessment Group (OPAG) for  
69 consideration in the last Planetary Science Decadal Survey (McKinnon et al.  
70 2009), but no such mission was formulated. With potential interest from  
71 international partners such as the European Space Agency (European Space Agency  
72 2021), there is potential scope for combining resources from agencies to achieve  
73 flagship-level science with more modest missions. This article specifically  
74 presents the case for a potential US-only New Frontiers-class mission.

75 2 *The need for a mid-scale Uranus orbiter mission*

Voyager 2's brief encounter with Uranus provided a tantalizing glimpse of the complexity and uniqueness of the planet and its wider system of rings and satellites, but ultimately supplied many more questions (e.g., Stone & Miner 1986; Arridge et al. 2014; Beddingfield et al. 2021). The currently limited understanding of Uranus is analogous to that of other planets after our initial flyby encounters (e.g., the Mariner missions to Mercury, Venus, and Mars; the Pioneer and Voyager missions to Jupiter and Saturn). Just as our understanding of those planets was transformed after sending dedicated orbiter missions (e.g., MESSENGER (Solomon et al. 2019), Pioneer Venus Orbiter (Colin 1980), the Viking missions (Soffen et al. 1976), Galileo (Johnson et al. 1992), Juno (Bolton et al. 2017), Cassini (Spilker 2019)), so too will our knowledge of Uranus expand tremendously from such long-term measurements and investigations. In particular, magnetospheric and atmospheric conditions can change rapidly compared to interior or surface conditions of the planet and satellites. For example, due to its unique extreme dipole tilt, the entire configuration of the Uranian magnetosphere varies drastically in a single (17.-hr) Uranian day; likewise, many plasma transport processes at play in the magnetosphere occur on the timescales of minutes or hours (e.g., injections, particle drifts, etc.). Furthermore, because observed changes in in-situ conditions may be the result of time-dependent dynamic processes or transition of the spacecraft into a different region of space, flybys are limited to snapshots of a planetary space environment. A similar case can be made for the atmospheric phenomena, which display a range of timescales, from hours (the eruption of convective plumes and interactions with the surrounding zonal winds; de Pater et al. 2015), to weeks (the evolution of rare dark ovals; Hammel et al. 2009), to years (the development of polar aerosol collars and caps, and associated changes in the polar windfield, Sromovsky et al., 2019). The only way to address this issue is with an orbiting spacecraft, as demonstrated by the results from previous orbital missions.

The first orbiters at every other planetary system also revealed many surprises that were not expected from the limited information gleaned by the flyby encounters of their predecessors. For example, one of the greatest discoveries of Cassini was the eruption of material from the subsurface ocean of Enceladus (Dougherty et al. 2006; Porco et al. 2006), a phenomenon unnoticed by the previous flybys of Pioneer 11 and the Voyagers. Future missions should yield similarly surprising results, especially given that the flyby measurements from Voyager 2 at Uranus may not have been representative (Kollmann et al. 2020). Thus, any orbiter mission at Uranus could be expected to provide a

114 substantial advancement in our understanding of the system relative to the  
115 Voyager 2 flyby. While a New Frontiers-class Uranus orbiter mission may not  
116 result in investigations as comprehensive as larger-class missions like Cassini  
117 at Saturn or Galileo at Jupiter, successful and transformative smaller-class  
118 missions (e.g., MESSENGER at Mercury and Juno at Jupiter) highlight the  
119 significant advancement in understanding of systems that can be obtained by  
120 targeted orbital missions.

121 Additionally, information on whether the classical Uranian satellites are  
122 ocean worlds provides direct complements to investigations of the New Horizons,  
123 Europa Clipper, and JUICE missions. Finally, perhaps most significantly, a New  
124 Frontiers-class Uranus orbiter mission would complement any potential mission  
125 to the Neptune system (e.g., Rymer et al. 2021) by providing additional  
126 information about both Ice Giant planets and thus enabling comparisons and  
127 contrasts between the two planets and their systems. There is also strong  
128 interest from the international community for collaboration on such a mission  
129 (Arridge et al. 2012; Fletcher et al. 2020a; Blanc et al. 2021; European Space  
130 Agency 2021).

131 It is unclear whether a large-scale strategic mission would be able to make  
132 the 2030–2034 launch window needed to take advantage of a Jupiter gravity assist  
133 to reach Uranus before it reaches equinox in 2050; after 2050, the northern  
134 hemispheres of the satellites not imaged by Voyager 2 will gradually recede  
135 into darkness and the magnetospheric configuration will again evolve back  
136 towards what was observed by Voyager 2. The timeliness of a Uranus orbiter  
137 mission is a primary motivation for evaluating what science can be done with a  
138 lower-cost, faster-turnaround mission within the New Frontiers class. To  
139 maximize the prospects of meeting launch opportunities by 2034, this mission  
140 concept omits scientific objectives that are only achievable by an atmospheric  
141 probe (e.g., Orton et al., 2021) and focus instead on the excellence of the  
142 achievable science in the broader Uranian system as well as cross-cutting  
143 heliophysics and astrophysics opportunities (e.g., Cohen & Rymer 2020).

144 Previous studies of potential future Uranus missions have been conducted and  
145 outlined the broad science that should be targeted by a large strategic mission  
146 (e.g., Hofstadter et al., 2019). These provide a solid foundation from which to  
147 focus a smaller-class New Frontiers mission, but have made assumptions about  
148 multiple aspects of the mission design (i.e., communications, power, orbit and  
149 spacecraft design) that may not be applicable or appropriate for a lower-cost  
150 mission. To date, no NASA-funded study has explored the trades necessary to  
151 construct a mission with high science return for <\$1B, though many such concepts

152 have been proposed (e.g., Elder et al. 2018; Jarmak et al. 2020; Leonard et al.  
153 2021).

154 In 2010, an Ice Giants mission concept study was conducted for the Planetary  
155 Science Decadal Survey (Hubbard 2010). The aim of this study was "to define a  
156 preferred concept approach along with the risk/cost trade space for a Uranus or  
157 Neptune Mission launched in the 2020–2023 timeframe and within a cost range of  
158 \$1.5B–\$1.9B in FY15\$". Though the study "developed a concept that can achieve  
159 very robust science at Uranus at a cost below flagship mission levels", the  
160 target cost range was ~50% higher than the modern NF cost cap. Notably, the use  
161 of a Jupiter gravity assist was not considered in this study because of the  
162 unfavorable trajectories during the targeted launch window. Ultimately, the  
163 study concluded that the identified science objectives could be achieved for  
164 \$1.894B (FY15\$), including an enhanced orbiter payload and six-month satellite  
165 tour, use of a solar electric propulsion (SEP) stage, and delivery of a 127-kg  
166 atmospheric entry probe. The "Uranus Orbiter and Probe" mission that resulted  
167 from this study was ranked as the third-highest-priority large-class mission in  
168 the 2011 Planetary Science Decadal Survey (National Research Council 2011).

169 A more recent Ice Giants Pre-Decadal Survey Mission Study was conducted  
170 looking at potential mission architectures to both Uranus and Neptune  
171 (Hofstadter et al. 2017; Hofstadter et al. 2019). Unlike its 2010 predecessor,  
172 this study targeted launch dates within the purview of the 2023 Planetary  
173 Science Decadal Survey (i.e., 2024–2037) and was charged to "[i]dentify missions  
174 across a range of price points, with a full life cycle cost not to exceed \$2B  
175 (FY15\$)" with no identified lower cost limit. Although the Science Definition  
176 Team explored over thirty architectures, neither a strawman payload was  
177 recommended nor was any explicit effort made to explore the New Frontiers trade-  
178 space. The lowest-cost option given a fully refined point design was a Uranus  
179 flyby that cost nearly \$1.5B (FY15\$); the Uranus orbiter point design with the  
180 lowest cost (\$1.7B FY15\$) carried an atmospheric probe and only a ~50-kg orbiter  
181 payload. Furthermore, the 2018 Decadal Survey mid-term review found "[t]he  
182 objectives of the mission concept described in the 2017 ice giants predecadal  
183 study have been changed significantly from the original *Vision and Voyages*  
184 science objectives", prompting a recommendation that "NASA should perform a new  
185 mission study based on the original ice giants science objectives identified in  
186 *Vision and Voyages* to determine if a more broad-based set of science objectives  
187 can be met within a \$2 billion cost cap." (National Research Council 2018).

189       The “proto” Science Traceability Matrix (STM) in Figure 1 summarizes a broad  
190       array of potential science objectives and outstanding mysteries, covering all  
191       areas of the system (satellites, magnetosphere, atmosphere, interior, and  
192       rings). These potential science objectives generally align with those of the  
193       Uranus Orbiter & Probe mission recommended in the 2013 Planetary Science Decadal  
194       Survey. Overall, the mission aims to address the overarching science goal to  
195       “*Explore the Uranian system to solve known mysteries and address*  
196       *multidisciplinary objectives relevant to the rings, satellites, magnetosphere,*  
197       *interior, and atmosphere.*” Measurement types (denoted in matrix form with a key  
198       at the bottom) are also provided for each objective.

	<b>Outstanding Mystery</b>	<b>Science Objective (Relevant V&amp;V Science Goal)</b>	<b>Potential Observables</b>
SATELLITES	<i>Do any of Uranus' classical satellites sustain a subsurface ocean?</i>	Determine whether the classical Uranian satellites have signatures indicative of subsurface oceans. (6)	<ul style="list-style-type: none"> <li>Tectonic and geomorphologic structures, tidal flexing, plume activity, physical libration, and thermal anomalies</li> <li>Topography</li> <li>Spectroscopic indications of outsourcing from interior</li> <li>Induced magnetic field and satellite tidal number/degree of compensation</li> </ul>
	<i>Which processes formed the extremely dark and resurfaced terrains of the five classical Uranian satellites?</i>	Determine the surface compositions of the classical Uranian satellites. (4)	<ul style="list-style-type: none"> <li>Compositional mapping and associations (or lack) with geologic features/topographic lows</li> <li>Regional distributions (leading versus trailing hemisphere) of dark material</li> <li>Compositional trends with distance from Uranus</li> </ul>
MAGNETOSPHERE		Understand what processes formed and modify the surfaces of the classical Uranian satellites. (4 & 5)	<ul style="list-style-type: none"> <li>Units and surface features/structures</li> <li>Topography and stratigraphy</li> <li>Relative age of units and features (estimated from cross-cutting relations and crater density)</li> <li>Incident plasma and energetic particle spectra (moon-magnetosphere interactions)</li> </ul>
	<i>How does plasma transport work in Uranus' unique magnetospheric configuration?</i>	Understand the fundamental structure and dynamics of Uranus' magnetosphere and the importance of internal versus external drivers. (1 & 3)	<ul style="list-style-type: none"> <li>Temporal and spatial variabilities in plasma and magnetic fields</li> <li>Plasma and energetic ion composition</li> <li>Particle energization and acceleration</li> <li>Times, durations and depths of satellite/ring microsignatures</li> </ul>
INTERIOR	<i>How does Uranus generate such an intense electron radiation belt?</i>	Understand what processes generate Uranus' intense electron radiation belt. (1 & 3)	<ul style="list-style-type: none"> <li>Plasma and low-frequency waves and wave power distributions</li> <li>Plasma and energetic electron and ion pitch-angle distributions and energy spectra</li> </ul>
		Understand the configuration and evolution of Uranus' magnetic field. (1 & 3)	<ul style="list-style-type: none"> <li>Map of the intrinsic magnetic field, including spherical harmonic coefficients</li> <li>Temporal evolution of the intrinsic magnetic field</li> <li>Low-degree (&lt;10) odd and high degree (&gt;10) even gravitational harmonics</li> <li>Internal heat flux as a function of latitude</li> </ul>
	<i>How is Uranus' interior structured below the clouds and how does it behave?</i>	Determine the bulk composition and the distribution of materials within Uranus. (1 & 2)	<ul style="list-style-type: none"> <li>Noble gas abundances (incl. He) – requires entry probe</li> <li>Bulk enrichments of C, N, and S (requires entry probe) and remote sensing above clouds</li> <li>Low-degree (&lt;10) even gravitational harmonics</li> <li>Map and temporal evolution of the intrinsic magnetic field</li> </ul>
ATMOSPHERE		Understand Uranus' global energy balance and internal heat flow. (1)	<ul style="list-style-type: none"> <li>Reflectivity at multiple phase angles and latitudes</li> <li>Thermal emission at multiple latitudes</li> <li>Temperature/density profiles</li> <li>Distribution of absorbers and temperature lapse rate in upper troposphere/stratosphere</li> </ul>
	<i>What mechanisms drive Uranus' large- and small-scale atmospheric dynamics?</i>	Understand Uranus' atmospheric heat transport mechanisms. (1 & 3)	<ul style="list-style-type: none"> <li>Mapping of entire planetary "surface"</li> <li>Upper atmospheric density and wave inventory</li> <li>Tracking of storms, clouds, and eddies in reflected sunlight</li> <li>Thermal profile, upward and downward radiative flux – requires entry probe</li> </ul>
		Understand Uranus' zonal and meridional circulation patterns. (1 & 3)	<ul style="list-style-type: none"> <li>Temperature and ortho/para-H<sub>2</sub> mapping</li> <li>Tracking of clouds</li> <li>3D maps of key volatiles and tracers (e.g., CH<sub>4</sub>, H<sub>2</sub>S, NH<sub>3</sub>, H<sub>2</sub>O, CO, para-H<sub>2</sub>)</li> <li>2-cm brightness temperature</li> </ul>
RINGS		Determine the thermodynamics and chemistry of Uranus' clouds and hazes. (1 & 3)	<ul style="list-style-type: none"> <li>Aerosol structure mapping</li> <li>3D maps of key volatiles and tracers (e.g., CH<sub>4</sub>, H<sub>2</sub>S, NH<sub>3</sub>, H<sub>2</sub>O, CO, para-H<sub>2</sub>)</li> <li>Abundances of hydrocarbons in upper atmosphere</li> </ul>
	<i>Why is the architecture of the Uranian ring-moon system so dynamically full and haphazard?</i>	Determine the processes that sculpt and maintain Uranus' ring-moon system. (1)	<ul style="list-style-type: none"> <li>Ring particle size distribution, planet/moon tidal parameters</li> <li>Ring internal structures (e.g., density waves and satellite wakes)</li> <li>Rings' non-circular shapes and pattern speeds</li> <li>Discovery of new moons and moon shapes, light-curves, and orbital elements</li> <li>Dusty ring spatial density and periodic structures</li> <li>Magnetic field orientation, components, and periodicities</li> </ul>
		Determine the composition and origin of Uranus' rings and small satellites. (1)	<ul style="list-style-type: none"> <li>Spectral absorption in moon and ring spectra</li> <li>Crater density on small moons</li> <li>Micrometeoroid impact flux and composition</li> <li>Radiation belt location and flux</li> </ul>

**Figure 1.** A summary of the outstanding science mysteries, science objectives (including linkages to the 2013 Planetary Science Decadal Survey goals), and potential observables that could be addressed by a future New Frontiers-class Uranus orbiter mission.

199        The science objectives presented here all address at least one of several  
 200 science goals for giant-planet system or satellite exploration outlined in the  
 201 2011 Planetary Science Decadal Survey (National Research Council 2011): 1) Giant  
 202 planets as ground truth for exoplanets; 2) Giant planets' role in promoting a  
 203 habitable planetary system; 3) Giant planets as laboratories for properties and  
 204 processes on Earth; 4) Formation and evolution of the satellites of the outer  
 205 solar system; 5) Processes controlling the present-day behavior of the  
 206 satellites of the outer solar system; and 6) Processes that result in habitable  
 207 environments. Each science objective's relevance to these overarching goals is  
 208 explicitly identified in Figure 1 along with potential observables.

Science Objective	Potential Measurement Types											
	Imaging/Spectroscopy				Gravity Science	Radio Occultations	Magnetic Field	Plasma	Energetic Particles	Plasma/low-frequency waves	Dust	In-situ atmospheric probe
	NIR	Thermal IR	Visible	UV								
Determine whether the classical Uranian satellites have signatures indicative of subsurface oceans.		X	X	X	X		X	X				
Determine the surface compositions of the classical Uranian satellites.	X	X	X									
Understand what processes formed & modify the surfaces of the classical Uranian satellites.	X	X	X					X	X			X
Understand how internal & external drivers generate plasma structures & transport within Uranus' magnetosphere.							X	X	X			
Understand what processes generate Uranus' intense electron radiation belt.							X	X	X	X		
Understand the configuration & evolution of Uranus' magnetic field.		X		X	X		X	X	X	X		
Determine the bulk composition & the distribution of materials within Uranus.		X	X		X	X	X			X		X
Understand Uranus' global energy balance & internal heat flow.	X	X	X		X	X	X					
Understand Uranus' atmospheric heat transport mechanisms.	X	X	x	X		X						X
Understand Uranus' zonal & meridional circulation patterns.	X	X	X	X	X	X	X					X
Determine the thermodynamics & chemistry of Uranus' clouds and hazes.	X	X	X	X		X			X			X
Determine the processes that sculpt & maintain Uranus' ring-moon system.	X		X	X	X	X	X	X	X			X
Determine the composition & origin of Uranus' rings & small satellites.	X	X	X	X				X	X			X

**Figure 2.** Mapping of the potential science objectives of a New Frontiers-class Uranus orbiter mission to different measurement types. This underscores the broad, cross-disciplinary science that can be achieved given that many instruments can provide observations relevant to multiple aspects of the science investigation.

Since the Uranian system provides a multitude of outstanding mysteries and unique characteristics to investigate, there are multiple possible complements of instruments that could deliver revolutionary science measurements as showcased in Figure 2. Despite the cost constraints, a New Frontiers-class Uranus orbiter mission is expected to achieve many of the science objectives outlined below.

### 3.1 Satellite Science

Determine whether the classical Uranian satellites have signatures indicative of subsurface oceans and determine their surface compositions. Uranus has five mid-sized classical satellites (Ariel, Miranda, Umbriel, Oberon, and Titania) in addition to its thirteen small moons. These moons have surface ices of common composition to those of the Pluto-Charon system - i.e., widespread H<sub>2</sub>O ice, CH<sub>4</sub> and other volatiles, hints of NH<sub>3</sub>-hydrates and the possible detection of tholins (Grundy et al. 2016; Cartwright et al. 2018; Schenk & Moore 2020). However, further investigation of these moons may provide insight on an icy evolution very different than those of Kuiper Belt Objects (KBOs), mainly due to the limited knowledge of CO<sub>2</sub> as a volatile ice at Uranus (Cartwright et al.

226 2015; 2020a), rather than carbon  
 227 monoxide on KBOs (Grundy et al.  
 228 2020). The widespread evidence  
 229 for resurfaced terrains from  
 230 tectonism and cryovolcanism on  
 231 the classical Uranian  
 232 satellites, hypothesized global  
 233 heating events, and the possible  
 234 presence of NH<sub>3</sub>-hydrates on  
 235 their surfaces indicate that  
 236 these moons are possible ocean  
 237 worlds (Hendrix et al. 2019;  
 238 Schenk & Moore 2020; Ćuk et al.  
 239 2020, Beddingfield & Cartwright  
 240 2021; Cartwright et al. 2021).  
 241 Heat flux estimates for Miranda  
 242 (Beddingfield et al. 2015) and  
 243 Ariel (Peterson et al. 2015)  
 244 indicate that these moons  
 245 experienced heating events in  
 246 the past (Ćuk et al. 2020),  
 247 possibly sustaining subsurface  
 248 liquid water. For example, the  
 249 estimated heat flux in the past  
 250 on Miranda is broadly consistent  
 251 with the heat flux generated by  
 252 Europa's current orbital  
 253 resonance (Hussman et al. 2002;  
 254 Ruiz et al. 2005). In addition, ground-based spectroscopic observations of the  
 255 Uranian satellites hint at the presence of ammonia-bearing species on the  
 256 surfaces of these moons (Bauer et al. 2002; Cartwright et al. 2018; 2020b). If  
 257 present in the lithosphere, ammonia-rich material would dramatically lower the  
 258 interior freezing temperature (compared to pure H<sub>2</sub>O ice), assisting in the  
 259 sustainability of subsurface oceans. If oceans are present in these satellites'  
 260 interiors, either globally or locally, they may have interacted, or currently  
 261 interact with the surface in the form of plumes, cryovolcanic flows, and/or  
 262 tectonic features indicative of nonsynchronous rotation. Images of the satellite  
 263 surfaces can be used to obtain surface compositions indicative of subsurface

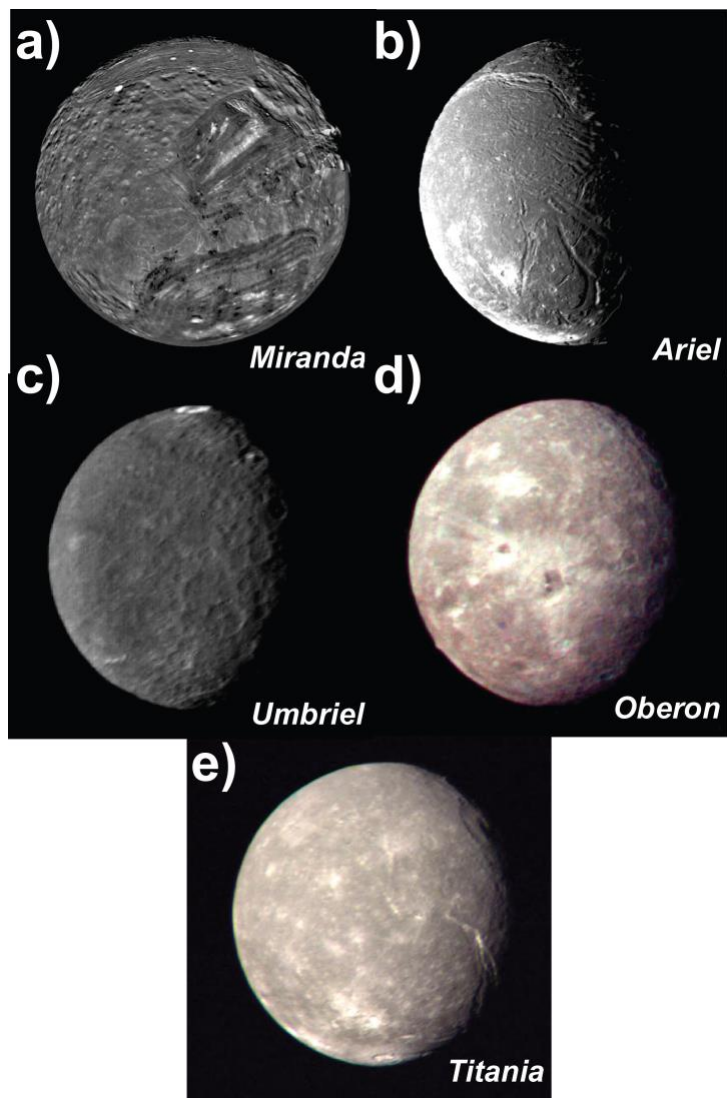


**Figure 3.** Voyager 2 images revealed surface features that have raised multiple mysteries regarding the composition, evolution, formation, and structure of the classical Uranian satellites. (Images from NASA/JPL)

255  
 256  
 257  
 258  
 259  
 260  
 261  
 262  
 263

264 ocean-surface interaction (infrared) and topographic information to investigate  
265 tectonics and geodynamics associated with a subsurface ocean, as well as map  
266 and analyze geologic units and surface features (visible). Observations of an  
267 induced magnetic field associated with any of the moons would also be indicative  
268 of a subsurface ocean (e.g., Arridge & Eggington, 2021; Weiss et al. 2021).

269 Understand what processes formed and modify the surfaces of the classical  
270 Uranian satellites. The geologic processes operating on the Uranian satellites  
271 are complex, as indicated by large tectonic and possibly cryovolcanic features  
272 imaged by Voyager 2 (Schenk 1991; Beddingfield & Cartwright, 2020; 2021; Schenk  
273 & Moore 2021). On Miranda and Ariel, tectonic and possibly cryovolcanic features  
274 extend well past the terminator in the Voyager 2 imaging dataset, as revealed  
275 by enhanced nightside "Uranus-shine" processing techniques (Stryke & Stooke  
276 2008). Miranda (Figure 3a) exhibits three unique "coronae", large polygonal  
277 shaped regions of deformed surface containing subparallel ridges and troughs  
278 that are highlighted by high and low albedos. These are made up of complex sets  
279 of tectonic features (Smith et al. 1986; Schenk 1991; Pappalardo et al. 1997)  
280 and may also contain cryovolcanic flows in one corona (Jankowski & Squyres 1988;  
281 Beddingfield & Cartwright, 2020) and the large Global Rift System cuts across  
282 the ancient cratered terrain. Ariel (Figure 3b) exhibits complex canyon systems,  
283 which are thought to be a result of internal processes driving tectonism  
284 (Johnson et al. 1987; Croft & Soderblom 1991), and possible cryovolcanic  
285 features including lobate flow-like features and double ridges (Beddingfield &  
286 Cartwright, 2021). Umbriel, Oberon, and Titania (Figures 3c-e) also exhibit  
287 large canyons, similar to those seen on some icy satellites elsewhere. However,  
288 the formation of these features is not well understood, and various mechanisms  
289 have been proposed (McKinnon 1988; McKinnon et al. 1991; Greenberg et al. 1991;  
290 Janes & Melosh 1988; Sori et al., 2017), which can only be tested through  
291 investigations such as mapping of surface features, compositions, and cratering  
292 densities, and obtaining topographic information from visible images. These  
293 images can also be used to map and analyze geologic units and surface features  
294 and compare them with weathering patterns to be expected from different plasma,  
295 particle or dust populations (e.g., Hendrix et al. 2012; Cartwright et al.  
296 2015). They can also be used to perform crater density studies to estimate  
297 surface ages. Compositional trends and regolith properties can be investigated  
298 using infrared spectra, providing key insight into the origin of the mysterious  
299 dark material. Since spectra depend both on surface composition and grain size  
300 (e.g., Hapke 2012), independent information on energetic particles is needed  
301 that affect grain size (e.g., Raut et al. 2008; Howett et al., 2020) and can

302 drive the chemical formation of the dark material (e.g., Lanzerotti et al. 1984)  
303 or other changes in color (e.g., Stephan et al. 2010; Hibbits et al. 2019).

304 *3.2 Magnetospheric Science*

305 Understand how internal & external drivers generate plasma structures and  
306 transport within Uranus' magnetosphere. The magnetosphere of Uranus (Stone &  
307 Miner 1986; Paty et al. 2020) offers a unique configuration that provides an  
308 opportunity to understand the drivers of magnetospheric dynamics throughout the  
309 solar system. With the planetary rotation axis tilted by 98° relative to the  
310 ecliptic plane and a magnetic field axis tilted by ~59° with respect to Uranus'  
311 rotation axis, the orientation of the magnetic field (Figure 4a) presents an  
312 asymmetrical obstacle to the impinging solar wind (Cao & Paty 2017; Paty et al.  
313 2020), which changes continuously during the 17.2-h Uranian day. Furthermore,  
314 the Uranian magnetic field requires higher-degree multipoles near the planet to  
315 adequately model the internal planetary field. This multipolar structure sets  
316 Uranus and Neptune apart from the Gas Giants, Jupiter and Saturn (e.g., Stanley  
317 & Bloxham 2006; Soderlund & Stanley 2020; Paty et al. 2020).

318 Plasma transport within a planetary magnetosphere may generally be driven by  
319 external and/or internal forces. External forcing would suggest that Uranus'  
320 magnetosphere becomes connected to the solar wind, whereas an internally-driven  
321 system would be subjected to centrifugal forces as the plasma is accelerated  
322 and energized. The magnetospheres of terrestrial planets with an intrinsic  
323 magnetic field (i.e., Earth and Mercury) are primarily driven by solar wind  
324 forcing, whereas the magnetospheres of gas giants Jupiter and Saturn are  
325 dominated by forces driven by internal plasma sources and fast planetary  
326 rotation. Voyager 2 observations suggest that Uranus may be solar wind-driven  
327 (Mauk et al. 1987). However, this runs contrary to Voyager 2 observations that  
328 revealed an apparent lack of solar wind alpha particles at higher energies  
329 (Krimigis et al. 1986); future measurements of suprathermal particle populations  
330 may yet reveal them. Given the unique combination of its extreme obliquity and  
331 the large offset of its magnetic field, Uranus' magnetic configuration varies  
332 between open and closed to the solar wind over a relatively fast (17.2-hr)  
333 Uranian day; this suggests that internal drivers must play a role, even though  
334 plasma transport due to the solar wind is decoupled from that due to rotation  
335 near the solstices (Selesnik & Richardson 1986; Vasyliunas 1986). Depending  
336 where Uranus is in its orbit, the solar wind would approach along the direction  
337 of the rotation axis, or perpendicular to it (or somewhere in between) because  
338 Uranus' rotation axis is almost aligned with its orbital plane. This will have  
339 a strong effect on the interaction of the solar wind plasma with the

340 magnetosphere of Uranus and the  
 341 resulting current system. A mission  
 342 arriving within a decade of 2050 would  
 343 have the chance to observe a very  
 344 different configuration relative to  
 345 the solar wind than Voyager 2 as the  
 346 alignment of the planet's rotation  
 347 axis changes seasonally, and thus may  
 348 expect to observed very different  
 349 magnetospheric dynamics.

350 Understand what processes generate  
 351 Uranus' intense electron radiation  
 352 belt. Planetary radiation belts  
 353 provide an in-situ laboratory to study  
 354 the universal process of particle  
 355 acceleration, providing conditions  
 356 that are hard to reproduce on Earth  
 357 and remain inaccessible in  
 358 astrophysical phenomena. Radiation  
 359 belts magnetically trap and energize  
 360 charged particles around a planet and  
 361 are as diverse as the planets they  
 362 encompass. Uranus' radiation belts  
 363 are especially interesting as Voyager  
 364 observations did not confirm our  
 365 expectations (Kollmann et al. 2020;  
 366 Paty et al. 2020). For the particles  
 367 to accumulate to high intensities, the  
 368 radiation belts need to draw from a  
 369 large reservoir of lower energy plasma  
 370 (as illustrated in Figure 4b) and/or  
 371 lose the accelerated particles very  
 372 slowly. Neither appeared to be the  
 373 case at Uranus, which features an  
 374 almost particle-free "vacuum"  
 375 magnetosphere with little source plasma to be accelerated (McNutt et al., 1987),  
 376 slow acceleration through radial diffusion (Cheng et al., 1987), and where waves  
 377 are thought to result mostly in particle losses (Coroniti et al., 1987). Thus,

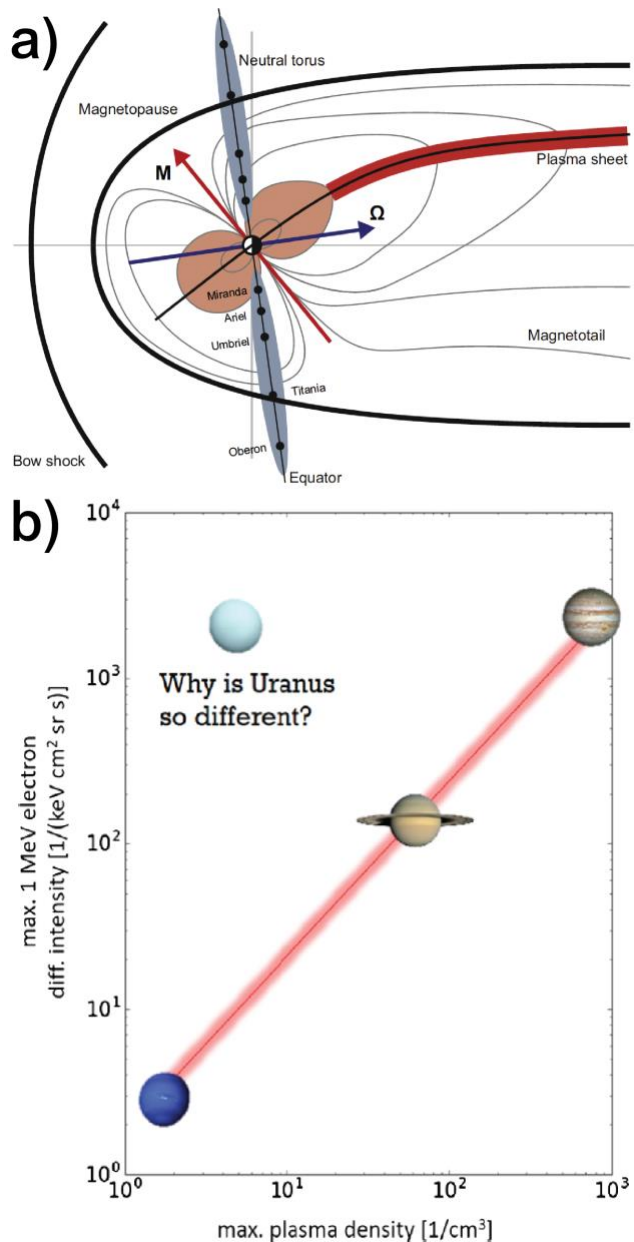


**Figure 4.** Uranus' asymmetric magnetosphere (a, from Arridge et al. 2014) presents a unique opportunity to test our understanding of magnetospheric physics. In particular, it remains unclear how and why the relationship between Uranus' 1 MeV electron intensities and the amount of potential source plasma in its magnetosphere stands out so starkly from the rest of the Giant planets (b, from Kollmann et al. 2020).

378 it remains a mystery why Uranus' electron belts appear surprisingly intense  
379 (e.g., compared to Saturn & Neptune (Mauk & Fox 2010)) whereas its ion belts  
380 show low intensities, despite sharing several physical processes (Mauk 2014).  
381

382 Wave observations may hold the key to a possible explanation, as the  
383 whistler-mode hiss and chorus wave intensities that Voyager 2 measured at Uranus  
384 were surprisingly higher than those it observed at any other planet (Kurth &  
385 Gurnett 1991); this suggests that such waves may play an important role in the  
386 system. In general, whistler-mode waves may play a role in both electron  
387 acceleration and loss, depending on the specific plasma conditions, a fact that  
388 has been of increasing interest (e.g., Thorne et al. 2013; Allison et al. 2019).  
389 Past studies at Uranus have suggested that the waves are causing a net loss  
390 (Tripathi & Singhal 2008), yet results may be biased by the limited temporal  
391 and spatial coverage of the available Voyager 2 measurements. A very different  
392 explanation why Uranus may behave so unexpectedly is because its unique  
393 magnetospheric configuration results in the dominance of processes that have  
394 been observed to play lesser roles at other planets. For example, the non-  
395 dipolar field near the planet could trap charged secondaries from cosmic rays  
396 hitting the atmosphere, which does not occur in other planets' more dipolar  
397 fields (Kollmann et al. 2020).

### 397 3.3 Interior Science

398 Understand the configuration & evolution of Uranus' magnetic field. Voyager 2  
399 showed that the intrinsic magnetic field of Uranus is multipolar (i.e., not  
400 dominated by the dipole component) and has no symmetries along any axis (e.g.,  
401 the dipole is tilted by 59° relative to the rotational axis, as previously  
402 mentioned (Figures 4a and 5a; Holme & Bloxham 1996; Soderlund & Stanley 2021)).  
403 Magnetic field measurements during the Voyager 2 flyby in combination with  
404 auroral observations allowed the large-scale field to be estimated up to  
405 spherical harmonic degree  $l=4$  (Herbert 2009); in contrast, the dipole-dominated  
406 magnetic fields of Jupiter and Saturn are known to  $l>10$  and surprises such as  
407 the north-south asymmetry and temporal variability of the Jovian field were  
408 discovered as they were characterized in greater detail (Cao et al. 2019;  
409 Connerney et al. 2021). Even more discovery awaits at Uranus (and Neptune) where  
410 the magnetic field is more spatially, and likely temporally, complex. Long-term  
411 in-situ measurements of the local magnetic field as well as energetic particles  
412 tracing global field properties (e.g., location and field strength of the foot  
413 points of field lines) will resolve both large- and small-scale fields over  
414 time thus enabling characterization of Uranus' dynamo to a level commensurate  
415 with Jupiter and Saturn (Cao et al. 2019; Connerney et al. 2021), which would

416 not only test hypotheses for  
 417 how its multipolar magnetic  
 418 field is generated but also  
 419 help explain why the dynamos  
 420 of gas and ice giant planets  
 421 differ so substantially.  
 422 Potential explanations for  
 423 Uranus' unique magnetic field  
 424 configuration relate to the  
 425 presence of a deep stably-  
 426 stratified layer (e.g.,  
 427 Stanley & Bloxham 2004), the  
 428 relatively weak influence of  
 429 rotation on deep convective  
 430 flows (Soderlund et al.  
 431 2013), the interplay of  
 432 density versus electrical  
 433 conductivity variations with  
 434 depth (Soderlund & Stanley  
 435 2020), among others. Thus, in  
 436 addition to characterizing  
 437 the magnetic field, Uranus'  
 438 interior structure, composition, heat flow, and dynamics must also be determined  
 439 in order to resolve the mystery of how the dynamo operates.

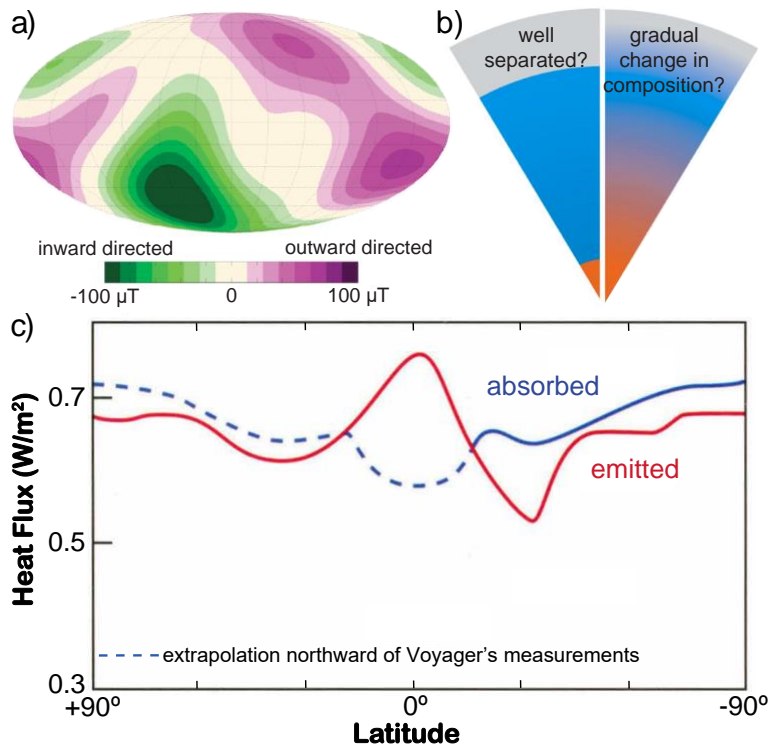


**Figure 5.** The peculiarities of Uranus' interior are showcased by the (a) multipolar intrinsic magnetic field, (b) unknown internal structure and bulk composition, and (c) energy balance with comparable absorbed and emitted heat fluxes. Adapted from Soderlund & Stanley (2020), Helled & Guillot (2017), and Ingersoll (1999), respectively.

Determine the bulk composition and the distribution of materials within Uranus. Standard three-layer structure models of Uranus infer that the planet consists of ~2 Earth masses of hydrogen-helium; although this estimate puts important limits on the planetary metallicity, it is not known which elements dominate the deep interior (Nettelmann et al. 2013; Helled & Fortney 2021; Teanby et al. 2021). Alternative structure models suggested that Uranus could have a density profile without discontinuities (Helled et al. 2011) and that a large fraction of water is not needed to fit the observed properties (Figure 5b). It is of particular importance to determine the global ice-to-rock ratio, which can also be used to address Uranus' formation – a long-standing problem for planet formation theory (Helled & Bodenheimer 2014; Helled et al. 2020; Mousis et al. 2021). Currently, the ice-to-rock ratio of Uranus remains only loosely constrained (Helled et al. 2011; Nettelmann et al. 2013). It is therefore clear that more accurate measurements of the gravity field and

454 estimates of the depth to the dynamo region from magnetic field measurements  
455 (e.g., Tsang & Jones 2020; Connerney et al. 2021; Masters & Soderlund 2022) are  
456 required to determine Uranus' bulk composition and its depth dependence.

457 Abundances of key species such as helium would tell us about the environment  
458 in which Uranus formed, and bulk enrichments of carbon, nitrogen, and sulfur  
459 would provide additional information on the planet formation process. However,  
460 it must again be noted that compositional determination can only be obtained by  
461 in-situ observations from an atmospheric probe, which is not considered within  
462 the scope of the New Frontiers-class orbiter mission promoted here due to cost  
463 cap limitations. Unfortunately, ground-based attempts to constrain aspects of  
464 the composition from measurements of atmospheric disequilibrium species (such  
465 as CO) have thus far been inconclusive (e.g., Cavalie et al. 2014).

466 Understand Uranus' global energy balance & internal heat flow. Uranus is the  
467 only outer planet in the solar system that is in approximate equilibrium with  
468 solar insolation (Pearl et al. 1990; Pearl & Conrath 1991), suggesting that its  
469 interior may not be fully convective and/or contains composition gradients that  
470 hinder convection (e.g., Nettelmann et al. 2016; Podolak et al. 2019; Scheibe  
471 et al. 2019; Vazan & Helled 2020), although atmospheric phenomena may also be  
472 responsible (Gierasch & Conrath 1987; Kurosaki & Ikoma 2017). Given the large  
473 uncertainties in the Voyager 2 measurements of Uranus' bond albedo and thermal  
474 emission, and the potential for temporal variability in the reflectivity and  
475 emission, a more precise energy balance measurement is necessary (Figure 5c).  
476 This requires mapping the reflectivity at multiple phase angles and latitudes  
477 (which can only be done with an orbiting spacecraft), and measuring the thermal  
478 emission at multiple latitudes. Furthermore, if convective inhibition is at  
479 play, then Uranus' internal heat flux may vary with time, and given that recent  
480 ground-based observations reveal many episodic convective events, an orbiter  
481 mission arriving during an active period may measure a higher heat flux.

482 Interior structure models use gravitational constraints to link planet  
483 composition, density, pressure, and temperature as a function of radius, albeit  
484 with non-unique solutions including 'hot' and 'cold' Uranus scenarios that may  
485 or may not be fully adiabatic (Helled et al. 2011; Nettelmann et al., 2013;  
486 Bethkenhagen et al. 2017; Podolak et al. 2019). As a result, improved  
487 measurements of the planet's composition, luminosity, and gravity field will  
488 reduce the uncertainty in interior heat flow. Moreover, variation of electrical  
489 conductivity with depth depends strongly on the planet's temperature structure,  
490 leading to potential interactions between the zonal winds and magnetic field in  
491 the semiconducting region of the atmosphere (Soyer et al. 2020). These

492 interactions are expected to produce perturbations in the poloidal magnetic  
493 field that may further test modeled temperature profiles (Soyer & Helled 2021).  
494

#### 494 3.4 Atmospheric Science

495 Understand Uranus' atmospheric heat transport mechanisms. Many atmospheric  
496 processes cause downward (e.g., solar insolation) and upward (e.g., thermal  
497 radiation, cumulus convection, and vertically propagating waves) radiation of  
498 energy. These processes provide local perturbations that shape atmospheric  
499 features such as cloud bands and vortices. Furthermore, the total upward heat  
500 flux in the atmosphere is the sum of such local processes. The connection  
501 between local atmospheric events and the global energy balance remains an  
502 outstanding question. Because the molecular weight of condensable species is  
503 heavier than the background hydrogen-helium atmospheric mixture, moist  
504 convection is generally inhibited and tends to happen in episodic bursts (Li &  
505 Ingersoll 2015; Friedson & Gonzales 2017; Leconte et al 2017; Li et al. 2018;  
506 Guillot 2021). Given this time-variability, a new mission may find that local  
507 episodic convection leads to a higher global heat flux. Even if a new mission  
508 arrives at a quiescent time, recent work presents specific testable predictions  
509 for the thermal stratification in observable layers during an inter-storm period  
510 (Li & Ingersoll 2015).

511 In the middle and upper atmosphere, our ignorance of heat transport processes  
512 is symptomized as the "energy crisis": Voyager 2 stellar occultations revealed  
513 that Uranus' thermosphere is hot (Broadfoot et al. 1986; Herbert et al. 1987;  
514 Stevens et al. 1993), although ground-based studies have revealed that these  
515 temperatures are declining over time (Melin, 2021). Although all four giant  
516 planets exhibit this "crisis", it is particularly surprising for Uranus because  
517 of its large axial tilt; given that the thermosphere is hot in both summer and  
518 winter hemispheres, solar heating cannot be the cause (Stevens et al. 1993).  
519 The vertical temperature gradient may point to the nature of the unknown heating  
520 (Clarke et al. 1987; Stevens et al. 1993; Waite et al. 1997; Raynaud et al.  
521 2003), but Voyager 2 occultations cannot distinguish between candidate heating  
522 mechanisms. New occultation measurements (including those relatively deep, down  
523 to several bars) with modern instrumentation from an orbiter should shed light  
524 on this long-standing mystery.

525 Understand Uranus' zonal and meridional circulation patterns. These  
526 circulations are critical for understanding the previously-discussed vertical  
527 heat transport and energy balance as well as producing a coherent model of  
528 atmospheric dynamics and how they extend into the interior (Hueso et al. 2021).  
529 Both Uranus' zonal wind profile (retrograde (westward) winds blowing at the

530 equator and a single prograde  
 531 (eastward) peak in each hemisphere),  
 532 and its tropospheric temperatures  
 533 (cool mid-latitudes contrasted with  
 534 a warm equator and pole), are in  
 535 stark contrast to the finely-banded  
 536 winds and temperatures of Jupiter  
 537 and Saturn. The penetration depth of  
 538 these winds is not well constrained,  
 539 but gravitational and ohmic  
 540 dissipation models suggest they are  
 541 limited to within the outermost 10%  
 542 of the planet (Kaspi et al. 2013;  
 543 Soyer et al. 2020) Uranus' winds  
 544 also exhibit a surprising  
 545 hemispheric asymmetry near the poles  
 546 (Sromovsky et al. 2014; Karkoschka  
 547 2015), which may be seasonally  
 548 driven. Whereas the cloud bands of  
 549 Jupiter and Saturn are loosely  
 550 associated with the zonal jets due  
 551 to eastward jet peaks acting as

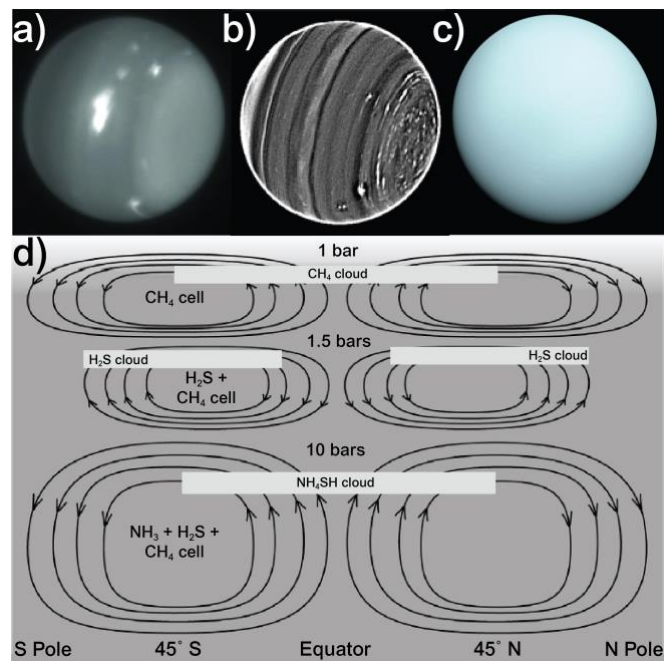


**Figure 6.** Remote observations of Uranus in the (a-b) near-infrared (from de Pater et al. 2015 and Sromovsky et al. 2015, respectively) have shown the Uranian atmosphere to be much more interesting than the (c) classic Voyager 2 image (NASA/JPL). It remains unclear whether (d) a three-layer overturning meridional circulation model accurately describes Uranus' zonal and meridional circulation patterns (adapted from Sromovsky et al. 2014).

552 transport barriers, Uranian cloud bands are seemingly not tied to the smooth  
 553 wind structure (Fletcher et al. 2020b), which may hint at unresolved peaks in  
 554 the zonal wind structure. Temporal tracking of cloud features in high-resolution  
 555 images would reveal any such peaks, as well as any seasonal changes since  
 556 Voyager 2.

557 The structure of Uranus' overturning meridional circulation remains unknown.  
 558 Depletion of gases such as methane (observed in the near-infrared) and  $\text{H}_2\text{S}$   
 559 (observed in the microwave) around the poles seems to suggest that Uranus has  
 560 a single deep circulation cell in each hemisphere, in which air rises from the  
 561 deep atmosphere at low latitudes, clouds condense out, and dry air is  
 562 transported to high latitudes where it descends (Sromovsky et al. 2015).  
 563 However, such a circulation pattern is inconsistent with observed cloud and  
 564 temperature distributions in the upper troposphere, implying that the meridional  
 565 circulation must be more complex, perhaps involving multiple stacked cells  
 566 (Figure 6d, Fletcher et al. 2020b). High-resolution maps of temperature and key  
 567 chemical tracers of vertical mixing are necessary to unravel the meridional

568 circulation. As for the Gas Giants, high-resolution measurements of the wind  
569 field may reveal coupling between zonal and meridional circulation via eddies  
570 (Salyk et al. 2006; Del Genio & Barbara 2012). This can be supported by remote  
571 microwave observations of H<sub>2</sub>S in the deep Uranian atmosphere (e.g., ALMA, VLA)  
572 (de Pater et al. 2021; Molter et al. 2021).

573 Determine the thermodynamics and chemistry of Uranus' clouds and hazes.  
574 During the *Voyager 2* flyby, Uranus appeared almost featureless. The subsequent  
575 presence of unexpected bright storms (Figure 5a; de Pater et al. 2015) has  
576 revealed that Uranus has an active, temporally dynamic, and poorly understood  
577 weather layer. Clouds and hazes occur preferentially at specific latitudes, and  
578 the banding pattern of tropospheric hazes is apparently not tied to the zonal  
579 wind structure. Vertically, clouds and tropospheric hazes are not found at the  
580 altitudes predicted by thermochemical models (de Pater et al. 1991); in fact,  
581 the compositions of Uranus' upper cloud layers remain unclear (Figure 5b;  
582 Sromovsky et al. 2015), although ices of H<sub>2</sub>S and CH<sub>4</sub> are promising candidates  
583 (Irwin et al. 2018). The thermodynamics and chemistry of the clouds have far-  
584 reaching implications for connecting the atmosphere to the planet's bulk  
585 composition, and for understanding the global energy balance (Moses et al.  
586 2021). A deeper understanding of cloud properties can be achieved with three-  
587 dimensional spectroscopic mapping of para-H<sub>2</sub>, CH<sub>4</sub>, H<sub>2</sub>S, and the spatial and  
588 vertical distributions of aerosols from near-infrared spectroscopy.

589 Voyager 2/UVS measurements (Broadfoot et al. 1986; Herbert et al. 1987;  
590 Bishop et al. 1990; Stevens et al. 1993) showed that Uranus' upper atmosphere  
591 was remarkably "clear", with hydrocarbon densities much lower than those found  
592 for any other giant planet (Melin 2021). Deeper in the stratosphere,  
593 hydrocarbons derived from methane photochemistry (Moses et al. 2021) are the  
594 main source of photochemical haze, act as continuum absorbers in the extreme  
595 ultraviolet, and serve as key tracers of vertical transport. For example, the  
596 spatial distribution of acetylene gas hints at a coupling between circulation  
597 patterns in the troposphere and stratosphere (Roman et al. 2020). Better  
598 constraints on their distributions can be determined by solar and stellar  
599 ultraviolet occultations (Smith & Hunten 1990; Herbert & Sandel 1998). A future  
600 New Frontiers-class orbiter mission could potentially host a breadth of multi-  
601 wavelength remote sensing instruments to optimizing its capability to addressing  
602 the science objectives in Figure 1.

### 603 3.5 Ring Science

604 Determine the processes that sculpt and maintain Uranus' ring-moon system.  
605 Since their discovery (Elliot et al. 1977), scientists have puzzled over how

606 the Uranian rings maintain  
 607 their narrow and non-circular  
 608 structures (French et al.  
 609 1991) but sometimes also show  
 610 striking changes (de Pater et  
 611 al., 2007). Voyager 2 and  
 612 Earth-based observations  
 613 have revealed that Uranus  
 614 hosts a system of dense  
 615 narrow rings lacking  
 616 meaningful spacing, diverse  
 617 broad and finely structured  
 618 dusty rings, and the most  
 619 tightly-packed system of  
 620 small moons in our solar  
 621 system (Figure 7; Nicholson  
 622 et al. 2018; Showalter 2021).

623 This "dynamically full"  
 624 system is known to be  
 625 unstable and is brimming with interesting interactions and dynamics including  
 626 overlapping resonant interactions between multiple moons (French et al. 2015).  
 627 The system is also "full" in the sense that it likely has no room for additional  
 628 moons, as multiple pairs are probable to cross orbits and collide in the near  
 629 future - in some cases, possibly as little as just thousands of years (French  
 630 & Showalter 2012). The ring-moon system contains important information about  
 631 its formation and evolution, and it can provide clues to the unique dynamical  
 632 history of Uranus (Ćuk et al. 2020; Hsu et al. 2021).

633 The most prominent features in the Uranian ring system are the ten narrow  
 634 and oddly-shaped main rings (French et al. 1988). Four of the main rings are  
 635 associated with resonances of small moons that likely play a role in shepherding  
 636 them (Porco & Goldreich 1987; Chancia et al. 2017). The mechanisms confining  
 637 the remaining ring edges and the nature of their present locations remain a  
 638 mystery (Esposito et al. 1991). We could further our understanding of how these  
 639 unique rings function by obtaining high-resolution images and occultation  
 640 profiles to reveal their detailed structures. These data could provide more  
 641 precise information on the rings' non-circular shapes, evidence of accretion  
 642 and/or fragmentation, density waves resulting from satellite resonances or  
 643 planetary interior oscillations, wakes of nearby satellites, and structures

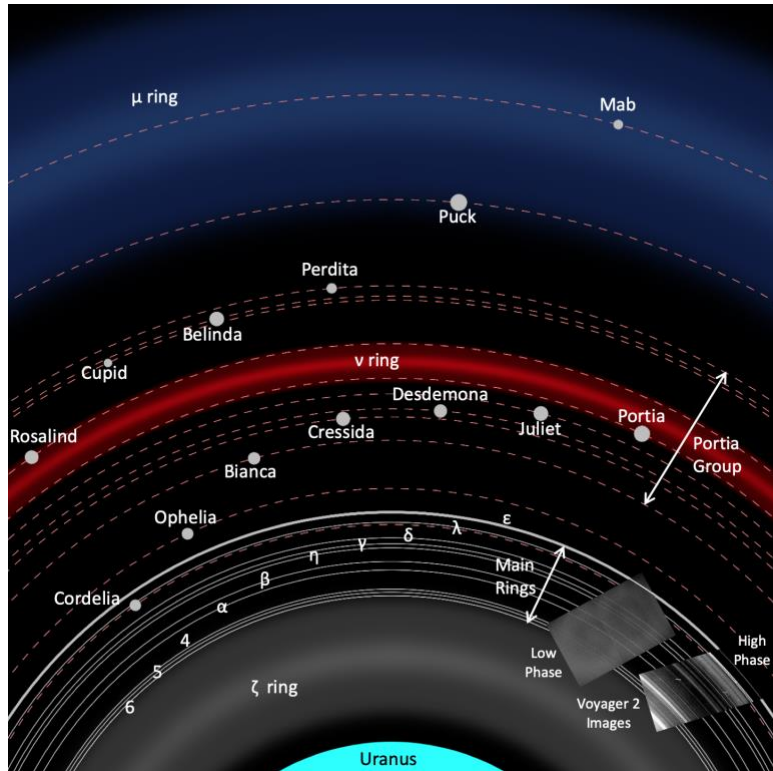


**Figure 7.** It remains unclear why the Uranian ring-moon system shown here is so dynamically full and apparently haphazard.

644 such as the propellers found in Saturn's rings (Tiscareno et al., 2008). There  
645 may also be undiscovered small moons we could detect and find to play a role in  
646 maintaining the narrow rings (Murray & Thompson 1990, Chancia & Hedman 2016).

647 Uranus also features a complex system of faint dusty rings (Ockert et al.  
648 1987; de Pater et al. 2006; Hedman & Chancia 2021). We know very little about  
649 the structures and properties of these dusty rings. They likely originate from  
650 micrometeoroid bombardment ejecta of the small inner moons and the dense rings  
651 themselves (Esposito & Colwell 1989). The ejecta then evolves under Uranus'  
652 oblateness, electric and various magnetic forces, and radiation pressure that  
653 will mostly affect the sub-micron grains (e.g., Juhaz & Horanyi 2002).  
654 Understanding the rates and sources of the dusty ring production and  
655 distribution throughout the system will help to determine the lifecycle of ring  
656 and moon material; this information is needed to understand the formation of  
657 the rings, their dynamics, and their current characteristics - including their  
658 differences in color (bluish for the  $\mu$ -ring and reddish for the others). This  
659 information requires high-phase-angle images of the dusty rings and high-  
660 resolution images of the small moons' surfaces for signs of cratering and  
661 accretion.

662 Thirteen small moons orbit between the main rings and the larger main moons  
663 of Uranus (Smith et al. 1986; Karkoschka 2001b; Showalter & Lissauer 2006).  
664 Nine of the moons' orbits are radially spaced within under 18,000 km. This  
665 arrangement is unstable on relatively short timescales and depends on the moons'  
666 unknown masses (Duncan & Lissauer 1997; French & Showalter 2012; French et al.  
667 2015). Many of these moons orbit inside Uranus' corotation radius. Thus, these  
668 moons' tidal interactions with Uranus cause inward migration towards the Roche  
669 limit, where they may fragment into new rings or interact with existing rings.  
670 They may also be driven outward through strong resonant torques if a more  
671 massive ring develops, like at Saturn (Charnoz et al. 2018. In this way, the  
672 ring-moon system may undergo recycling throughout its lifetime (Hesselbroek &  
673 Minton 2019). Determining how this process works is fundamental to understanding  
674 how planetary ring-moon systems operate under a variety of configurations.

675 Determine the composition and origin of Uranus' rings and small satellites.  
676 The rings and small moons of Uranus are dark, and their compositions are unknown  
677 (Karkoschka 2001). Observations (Grundy et al. 2006) have revealed H<sub>2</sub>O and CO<sub>2</sub>  
678 ice spectral features on Uranus' larger moons, whereas the rings' spectra are  
679 flat (de Kleer et al. 2013). Limited observations of the small moons have not  
680 revealed if they are more akin to the larger moons or the rings. Thus, improved  
681 near-infrared spectra of the small moons and rings are needed to determine both

682 their origins and the darkening mechanism(s) in the system. Observations of  
683 Uranus' unique magnetic field and magnetospheric particle environment would  
684 provide insight into the interaction between the plasma in Uranus' magnetosphere  
685 and the regoliths of its moons and ring particles and its potential to alter  
686 their compositions.

687 4 Required Mission Design Scope and Considerations

688 Although a New Frontiers-class orbiter mission would by definition likely  
689 achieve less science than those targeted by previously-studied large strategic-  
690 class missions, such a mission should put an emphasis on maintaining balance  
691 across the research disciplines as significant system science should be  
692 achievable. Results from previous larger studies suggest the feasibility of a  
693 New Frontiers-class orbiter mission to Uranus. For example, the costs in the  
694 Hubbard (2010) Decadal study suggest ~\$1.1B (FY15\$) for Phases A-D for an  
695 orbiter mission with a flagship-class payload without an atmospheric probe  
696 (assuming 30% reserves) without the launch vehicle costs. Appropriately scoping  
697 the payload to accommodate New Frontiers-class science would reduce both the  
698 payload and spacecraft costs. From a mission design standpoint, the potential  
699 use of a SEP stage with a cruise of ~14 years could reduce the spacecraft's  
700 chemical propulsion burden, while still leaving enough radioisotope power system  
701 (RPS) lifetime for the baseline mission, to be feasible within the New Frontiers  
702 cost cap. Furthermore, a New Frontiers-class Uranus orbiter mission could be  
703 implemented with current technologies, given appropriate trades in design and  
704 scope; however, multiple technologies under development could enhance and expand  
705 the scope and capability of such a mission (e.g., Spilker 2021).

706 Power is perhaps the most limiting constraint on a Uranus orbiter mission,  
707 and addressing power within cost is the primary obstacle to the feasibility of  
708 a New Frontiers-class Uranus orbiter mission. This plays into not only the  
709 extent of the payload and spacecraft subsystems, but also the power required  
710 for deep-space communications, specifically downlink. Previous Ice Giant  
711 mission studies (Hubbard 2010; Hofstader et al. 2017) have resulted in  
712 architectures requiring >350 W-e end-of-life power, which required three or  
713 more now-cancelled Enhanced Multi-Mission Radioisotope Thermoelectric  
714 Generators (eMMRTGs). Owing to the relative inefficiency and significant cost  
715 of current RPS, any design should attempt to reduce the needed end-of-life  
716 power; this will have significant impact on both the spacecraft and orbit design  
717 as well as the communication subsystem and payload. Hence, accelerating the  
718 development and expanding the efficiency and lifetime (and potentially reducing  
719 the cost) of next-generation RPS would significantly enhance the mission. For

Instrument Type	Representative Heritage Instrument	Mass (kg)	Power (W)
Wide-angle Camera	MESSENGER/MDIS [Hawkins et al. 2007]	4.6	10.0
Visible/Near-infrared Imaging Spectrometer	New Horizons/Ralph [Reuter et al. 2008] & Lucy/L'Ralph	19.0	7.1
Magnetometer	MESSENGER [Anderson et al. 2007]	4.7 (incl. boom)	4.2
Plasma Spectrometer	MESSENGER/FIPS (ions) [Andrews et al. 2007]	1.4	2.1
	Parker Solar Probe/SPAN-B (electrons) [Kasper et al. 2016]	2.5	2.0
Energetic Particle Sensor	Parker Solar Probe/EPI-Lo [McComas et al. 2017]	3.9	4.3
Ultra-stable Oscillator	New Horizons/REX [Tyler et al. 2008]	0.1	2.1
Narrow-angle Camera	New Horizons/LORRI [Cheng et al. 2007]	9.0	5.5
Ultraviolet Imaging Spectrometer	New Horizons/Alice [Stern et al. 2008b]	5.0	5.8
Thermal Infrared Imager	Lunar Reconnaissance Orbiter/Diviner [Paige et al. 2009]	11.5	18.4
		<b>TOTAL</b>	<b>52.1</b>
			<b>62</b>

**Figure 8.** Example of an instrument complement that would enable broad, cross-disciplinary science return for New Frontiers-class Uranus orbiter mission. White rows indicate a notional baseline payload that may be feasible given realistic cost and power constraints; gray rows provide additional high-impact instruments that could be included if resources and operations allow. Duty cycles and operations would be dependent on the mission and spacecraft designs.

example, the recent Neptune Odyssey mission concept uses three next-generation RPS (Rymer et al. 2021), suggesting that a New Frontiers-class Uranus mission could be implemented with fewer. This of course assumes that a sufficient supply of plutonium is available for future space exploration missions, which could potentially be achieved with early enough planning and investment (Zakrajsek 2021). It is also important to emphasize that future RPS needs may come from outside the Planetary Science community - e.g., the Heliophysics concept for an Interstellar Probe mission (Kinnison et al. 2021).

With current technology, a typical baseline New Frontiers-class Uranus orbiter mission would target a less than twelve-year cruise (potentially with a Centaur flyby en route to Uranus) and a two-year mission at Uranus with a system tour that enables surface mapping of the large satellites as well as spatial coverage of the planet, rings, and small moons; this baseline could be significantly lengthened if the lifetime of future RPS were improved. Previous studies (e.g., McAdams et al. 2011) have demonstrated that such short-duration trajectories are feasible.

Another significant driver is determining the total mass that can be put into Uranus orbit within the New Frontiers cost cap given the significant propellant required to achieve orbit insertion (approximately 3 kg of propellant required to deliver 1 kg of payload into orbit) and to maintain pointing for both downlink and targeting of scientific objectives, mass efficiency will be critical. This mission uses chemical propulsion, though an ion engine, like

742 that used on the Dawn mission, could be considered as a potential future trade;  
743 the use of a SEP stage, as has been explored by previous studies, could be  
744 considered, but would likely be difficult to fit within the New Frontiers cost  
745 cap. A realistic ~50-kg payload using current technologies would provide closure  
746 to numerous scientific mysteries summarized in Figure 1; however, cost and power  
747 limitations of course add additional limitations, though the latter could be  
748 addressed with a creative concept of operations that varies instrument duty  
749 cycles. A summary of a notional baseline payload and representative heritage  
750 instruments is presented in Figure 8. Because of the potential mass limitations,  
751 a New Frontiers-class Uranus orbiter is unlikely to have the resources to carry  
752 an atmospheric probe of the size and capability proposed by previous studies  
753 (e.g., Hubbard 2010; Hofstadter et al. 2017; Hofstadter et al. 2019) and that  
754 would fully obtain all of the potential observables listed in Table 1. However,  
755 such a mission might be able to consider inclusion of a smaller, more focused  
756 atmospheric probe (e.g., Sayanagi et al. 2020), which would likely be able to  
757 make a subset of the identified probe potential observables (e.g., thermal  
758 profile) in Table 1. Fortunately, cost reduction and increases in the capability  
759 and availability of launch vehicles (e.g., SLS) could significantly enhance the  
760 deliverable mass and thus scope of a New Frontiers-class Uranus orbiter mission,  
761 as well as potentially enabling contributed elements from other agencies, while  
762 also adding the capability to launch outside of windows with Jupiter gravity  
763 assists. Furthermore, the risk-versus-benefit of using aerocapture for orbit  
764 insertion should be analyzed as it can strongly increase the mass of the  
765 delivered payload and shorten flight times (Hall et al. 2005; Spilker et al.  
766 2016; Girija et al. 2020; Dutta et al. 2021).

767 Another primary design driver for a New Frontiers-class Uranus orbiter  
768 mission will be limitations on the total mission duration resulting from the  
769 nominal fourteen-year flight design life of currently-available RPS (Lee &  
770 Bairstow 2015); however, future RPS are targeting and recent pre-Decadal mission  
771 studies designed baseline missions based on longer lifetimes (e.g., Howett et  
772 al. 2021; Rymer et al. 2021). The preliminary design is a two-year baseline  
773 mission in orbit at Uranus with a system tour that enables sufficient surface  
774 mapping of the large satellites as well as imaging coverage of the planet, its  
775 rings, and the small moons. Furthermore, the mission will be designed to  
776 complete its baseline mission by Uranus spring equinox (2050), allowing for  
777 imaging of the northern hemispheres of the satellites that were not illuminated  
778 during the Voyager 2 flyby. This, of course, constrains the launch vehicle  
779 selection and propulsion. The initial assumption is that the spacecraft will be

780 designed to accommodate both three-axis and spin-stabilization to enable simpler  
781 operations during the long cruise, as was done on New Horizons (Stern 2008).

782 As previously discussed, the architecture summarized here does not include  
783 any mission critical technologies below TRL6 and baselines high-heritage  
784 instrumentation and spacecraft subsystems. However, the mission could benefit  
785 from significant enhancement by using aerocapture (TRL~3), which is under  
786 current NASA-funded development (Spilker et al. 2018). Likewise, any mission to  
787 Uranus will likely require a nuclear power system, though deep-space use of  
788 solar power could also be considered (e.g., Piszcior et al. 2008). The baseline  
789 mission can use currently-available MMRTGs (Lee & Bairstow 2015). However, the  
790 ability to use either the next-generation RTG (NG-RTG; Matthes et al. 2018) or  
791 the dynamic RPS (DRPS; Qualls et al. 2018) systems currently under development  
792 by NASA with estimated launch availability dates of 2026 and 2030, respectively  
793 - which were baselined for the recent Neptune Odyssey mission concept (Rymer et  
794 al. 2021) - would provide 20-380% greater end-of-life power than the MMRTGs and  
795 significantly enhance the capability of a New Frontiers-class Uranus orbiter.

## 796 5 Summary and Conclusion

797 Uranus presents a unique and tantalizing, yet woefully underexplored,  
798 destination due to the unique properties of it and its system and additionally  
799 provides an opportunity to explore the currently underexplored category of Ice  
800 Giants. Compelling characteristics of the Uranian system that are unlike other  
801 planets that have been studied in detail include: 1) five major satellites -  
802 potential ocean worlds with drastic surface features; 2) a unique magnetosphere  
803 with a dramatic configuration that features highly-tilted rotation and magnetic  
804 axes driven by a non-dipole-dominated interior dynamo as well as unexpectedly  
805 strong radiation belts and plasma wave activity; 3) a bulk planetary composition  
806 thought to be dominated by heavier "ices" (e.g., H<sub>2</sub>O, CH<sub>4</sub>, H<sub>2</sub>S, and NH<sub>3</sub>) and a  
807 poorly constrained amount of rocky material; 4) climate with unique atmospheric  
808 circulation, winds, chemistry, and cloud formation; and 5) a dynamically full  
809 and apparently haphazard ring-moon system.

810 As has been demonstrated by previous missions to other planets, orbiting  
811 missions are necessary to truly characterize a world, especially for  
812 magnetospheric and atmospheric studies focusing on processes with timescales  
813 shorter than or comparable to the duration of a flyby. Likewise, close periapse  
814 passes across a wide range of planetary latitudes and longitudes enabled by a  
815 sustained orbiter mission are required to intimately probe the interior of  
816 Uranus, which may hold keys to understanding the formation of our solar system  
817 as well as providing ground truths for the understanding of exoplanets with

818 similar mass and radii, and potentially those with similar chemical enrichments,  
819 axial tilts, low-temperature conditions, and higher-order magnetic fields. As  
820 such, exploration of Uranus will not only enhance our understanding of the Ice  
821 Giant planets themselves but also extends to planetary dynamics throughout our  
822 solar system and beyond.

823 While we are pushing the frontier of exploration further out within our solar  
824 system and discover more and more Ice Giant-sized exoplanets, a mission to  
825 Uranus is becoming timely. Because of the strong desire to revisit the Uranian  
826 system before the unimaged hemispheres of the satellites recede back into  
827 darkness (equinox is in early 2050), there is an imperative to explore any and  
828 all options. In particular, a mid-cost New Frontiers-class orbiter mission -  
829 such as the one described in this article - could achieve many significant and  
830 interdisciplinary system science questions with currently-available technology,  
831 if appropriate care is taken in the mission design. For example, the technical  
832 challenges of flying to and entering orbit around Uranus and sustaining  
833 operations at a distance of 20 AU must all be carefully considered and traded  
834 against the overall mission feasibility, impact, and cost. As this paper shows,  
835 a mid-scale (e.g., New Frontiers-class) mission could achieve significant and  
836 high-impact cross-disciplinary science observations using current technology.  
837

### 838 References

- 839 Allison, H., et al., 2019, On the Importance of Gradients in the Low-Energy  
840 Electron Phase Space Density for Relativistic Electron Acceleration, JGR,  
841 10.1029/2019JA026516
- 842 Anderson, B.J., Acuña, M.H., Lohr, D.A. et al. The Magnetometer Instrument on  
843 MESSENGER. *Space Sci Rev* 131, 417–450 (2007). doi:10.1007/s11214-007-9246-7
- 844 Andrews, G.B., Zurbuchen, T.H., Mauk, B.H. et al. The Energetic Particle and  
845 Plasma Spectrometer Instrument on the MESSENGER Spacecraft. *Space Sci Rev* 131,  
846 523–556 (2007). <https://doi.org/10.1007/s11214-007-9272-5>.
- 847 Arridge, C.S. and J.W.B. Egginton (2021) Electromagnetic induction in the icy  
848 satellites of Uranus, *Icarus*, 367, 114562, doi:10.1016/j.icarus.2021.114562
- 849 Arridge, C. S. et al. (2014), The science case for an orbital mission to Uranus:  
850 Exploring the origins and evolution of ice giant planets, *Planet. Space Sci.*,  
851 104, 122–140, doi:10.1016/j.pss.2014.08.009.
- 852 Arridge, C.S., Agnor, C.B., André, N. et al. (2012) Uranus Pathfinder: exploring  
853 the origins and evolution of Ice Giant planets. *Exp Astron* 33, 753–791.  
854 <https://doi.org/10.1007/s10686-011-9251-4>

- 855 Batalha, N. M. et al. (2011), Planetary Candidates Observed by Kepler. III.  
856 Analysis of the First 16 Months of Data, ApJS, 204, 24, doi:10.1088/0067-  
857 0049/204/2/24.
- 858 Bauer, J. M., et al (2002), The near infrared spectrum of Miranda: Evidence of  
859 crystalline water ice, Icarus, 158, 178-190, doi:10.1006/icar.2002.6876.
- 860 Beddingfield, C. B., & Cartwright, R. J. (2021). A lobate feature adjacent to  
861 a double ridge on Ariel: Formed by cryovolcanism or mass wasting?. Icarus,  
862 114583.
- 863 Beddingfield, C., Li, C., Atreya, S., Beauchamp, P., Cohen, I., Fortney, J., ...  
864 Showalter, M. (2021). Exploration of the Ice Giant Systems. *Bulletin of the*  
865 *AAS*, 53(4). <https://doi.org/10.3847/25c2cfab.e2bee91e>.
- 866 Beddingfield, C. B., & Cartwright, R. J. (2020). Hidden tectonism on Miranda's  
867 Elsinore Corona revealed by polygonal impact craters. Icarus, 343, 113687.
- 868 Beddingfield, C. B., et al. (2015), Fault geometries on Uranus' satellite  
869 Miranda: Implications for internal structure and heat flow, Icarus, 247, 35-  
870 52, doi:10.1016/j.icarus.2014.09.048.Bishop et al. 1990
- 871 Bethkenhagen, M., Meyer, E. R., Hamel, S., Nettelmann, N., French, M., Scheibe,  
872 L., ... & Redmer, R. (2017). Planetary ices and the linear mixing  
873 approximation. *The Astrophysical Journal*, 848(1), 67.
- 874 Blanc, M., Mandt, K., Mousis, O. et al. Science Goals and Mission Objectives  
875 for the Future Exploration of Ice Giants Systems: A Horizon 2061  
876 Perspective. *Space Sci Rev* 217, 3 (2021). <https://doi.org/10.1007/s11214-020-00769-5>
- 877 Bolton, S.J., Lunine, J., Stevenson, D. et al. The Juno Mission. *Space Sci Rev*  
879 213, 5-37 (2017). <https://doi.org/10.1007/s11214-017-0429-6>.
- 880 Broadfoot, A. Let al. (1986), Ultraviolet spectrometer observations of Uranus,  
881 *Science*, 233, 74-79, doi:10.1126/science.233.4759.74.
- 882 Cao H., Dougherty M.K., Hunt G.J., Provan G., Cowley S.W.H., Bunce E.J., Kellock  
883 S., Stevenson D.J. (2019), The landscape of Saturn's internal magnetic field  
884 from the Cassini Grand Finale. *Icarus* 344, 113541,  
885 doi:10.1016/j.icarus.2019.113541.
- 886 Cao, X., & C. Paty (2017), Diurnal and seasonal variability of Uranus's  
887 magnetosphere, *J. Geophys. Res. Space Physics*, 122, 6318-6331,  
888 doi:10.1002/2017JA024063.
- 889 Cartwright, R. J., et al (2021) The Science Case for Spacecraft Exploration of  
890 the Uranian Satellites: Candidate Ocean Worlds in an Ice Giant System *Planet.*  
891 *Sci. J.* 2 120, doi:10.3847/PSJ/abfe12.

892 Cartwright, R. J., Emery, J. P., Grundy, W. M., Cruikshank, D. P., Beddingfield,  
893 C. B., & Pinilla-Alonso, N. (2020a). Probing the regoliths of the classical  
894 Uranian satellites: Are their surfaces mantled by a layer of tiny H<sub>2</sub>O ice  
895 grains?. *Icarus*, 338, 113513, doi:10.1016/j.icarus.2019.113513.

896 Cartwright, R. J., Beddingfield, C. B., Nordheim, T. A., Roser, J., Grundy, W.  
897 M., Hand, K. P., ... & Scipioni, F. (2020b). Evidence for ammonia-bearing  
898 species on the Uranian satellite Ariel supports recent geologic activity. *The  
899 Astrophysical Journal Letters*, 898(1), L22.

900 Cartwright, R. J. et al. (2018), Red material on the large moons of Uranus:  
901 Dust from the irregular satellites?, *Icarus*, 314, 210-231,  
902 doi:10.1016/j.icarus.2018.06.004.

903 Cartwright, R. J., et al. (2015), Distribution of CO<sub>2</sub> ice on the large moons of  
904 Uranus and evidence for compositional stratification of their near-surfaces,  
905 *Icarus*, 257, 428-456, doi:10.1016/j.icarus.2015.05.020

906 Cavalie, T. et al. (2014), The first submillimeter observation of CO in the  
907 stratosphere of Uranus, *A&A*, 562, A33, doi:10.1051/0004-6361/201322297.

908 Chancia, R. O. & Hedman, M. M. (2016), Are there moonlets near the Uranian alpha  
909 and beta rings? *AJ*, 152, 211. doi:10.3847/0004-6256/152/6/211.

910 Chancia, R. O., et al. (2017), Weighing Uranus' Moon Cressida with the eta ring.  
911 *AJ*, 154, 153. doi:10.3847/1538-3881/aa880e.

912 Charnoz, S., et al. (2018), The Origin of Planetary Ring Systems, in *Planetary  
913 Ring Systems* (eds. M. S. Tiscareno and C. D. Murray), pp. 517-538. Cambridge  
914 University Press, doi:10.1017/9781316286791.018.

915 Cheng, A.F., Weaver, H.A., Conard, S.J. et al. Long-Range Reconnaissance Imager  
916 on New Horizons. *Space Sci Rev* 140, 189-215 (2008).  
917 <https://doi.org/10.1007/s11214-007-9271-6>

918 Cheng, A.F., S.M. Krimigis, B.H. Mauk, E.P. Keath, C.G. MacLennan, L.J.  
919 Lanzerotti, M.T. Paonessa, T.P. Armstrong, Energetic ion and electron phase  
920 space densities in the magnetosphere of Uranus. *J. Geophys. Res.*, 92(A13),  
921 15315-15328 (1987). <https://doi.org/10.1029/JA092iA13p15315>

922 Clarke, J. T. et al. (1987), The excitation of the far ultraviolet electroglow  
923 emissions on Uranus, Saturn, and Jupiter, *J. Geophys. Res.*, 92, A13, 15139-  
924 15147, doi:10.1029/JA092iA13p15139.

925 Cohen, Ian J. and Rymer Abigail M. (2020), Cross-NASA divisional relevance of an  
926 Ice Giant mission. *Phil. Trans. R. Soc. A.*, 378,  
927 <http://doi.org/10.1098/rsta.2020.0222>

928 Colin, L. (1980), The Pioneer Venus Program, *J. Geophys. Res.*, 85( A13), 7575-  
929 7598, doi:10.1029/JA085iA13p07575.

930 Connerney, J. E. P., Timmins, S., Oliversen, R. J., Espley, J. R., Joergensen,  
931 J. L., Kotsiaros, S., ... & Levin, S. M. (2021). A New Model of Jupiter's  
932 Magnetic Field at the Completion of Juno's Prime Mission. *Journal of*  
933 *Geophysical Research: Planets*, e2021JE007055.

934 Coroniti, F.V., W.S. Kurth, F.L. Scarf, S.M. Krimigis, C.F. Kennel, D.A.  
935 Gurnett, Whistler mode emissions in the Uranian radiation belts. *J. Geophys.*  
936 Res. 92(A13), 15234-15248 (1987). <https://doi.org/10.1029/JA092iA13p15234>

937 Croft, S. & L. Soderblom (1991) Geology of the uranusian satellites, in *Uranus*,  
938 Tucson, AZ: University of Arizona Press, pp. 561-628.

939 Cuk, M., et al. (2020), Dynamical History of the Uranian System. *Planet. Sci.*  
940 J., 1, 22, doi:10.3847/PSJ/ab9748.

941 de Kleer et al. (2013), Near-infrared spectra of the Uranian ring system,  
942 *Icarus*, 226, 1039-1044, doi:10.1016/j.icarus.2013.07.016.

943 de Pater, I., Moeckel, C., Tollefson, J., Butler, B., Kleer, K. de, Fletcher,  
944 L., ... Spilker, T. R. (2021). Prospects to study the Ice Giants with the  
945 ngVLA. *Bulletin of the AAS*, 53(4). <https://doi.org/10.3847/25c2cfab.029d5009>

946 de Pater, I., et al. (2015), Record-breaking storm activity on Uranus in 2014,  
947 *Icarus*, 252, 121-128, doi:10.1016/j.icarus.2014.12.037.

948 I. de Pater, H.B. Hammel, M.R. Showalter, M. van Dam (2007). The dark side of  
949 the rings of Uranus. *Science* 317, 1888-1890.

950 de Pater, I. et al. (2006), New Dust Belts of Uranus: One Ring, Two Ring, Red  
951 Ring, Blue Ring. *Science*, 312, 5770, 92-94, doi:10.1126/science.1125110.

952 de Pater, I. et al. (1991), Possible microwave absorption by H<sub>2</sub>S gas in Uranus'  
953 and Neptune's atmospheres, *Icarus*, 91, 2, 220-233, doi:10.1016/0019-  
954 1035(91)90020-T.

955 Del Genio, A. D. & J. M Barbara (2012), Constraints on Saturn's tropospheric  
956 general circulation from Cassini ISS images, *Icarus*, 219, 2, 689-700,  
957 doi:10.1016/j.icarus.2012.03.035.

958 Dougherty, M., et al. (2006), Identification of a Dynamic Atmosphere at  
959 Enceladus with the Cassini Magnetometer, *Science*, 311, 5766, 1406-1409,  
960 doi:10.1126/science.1120985.

961 Duncan, M. J. & J. J. Lissauer (1997), Orbital Stability of the Uranian Satellite  
962 System, *Icarus*, 125, 1-12, doi:10.1006/icar.1996.5568.

963 Dutta, S., et al. (2021). Aerocapture as an Enhancing Option for Ice Giants  
964 Missions. *Bulletin of the AAS*, 53(4). doi:10.3847/25c2cfab.e8e49d0e.

965 Elder, C. M., et al. (2018). OCEANUS: A high science return Uranus orbiter with  
966 a low-cost instrument suite. *Acta Astr.*, 148, 1-11,  
967 doi:10.1016/j.actaastro.2018.04.019.

- 968 Elliot, J. L., et al (1977), The rings of Uranus, *Nature*, 267, 328-330,  
969 doi:10.1038/267328a0.
- 970 Esposito, L. W. et al. (1991). Particle properties and processes in Uranus'  
971 rings. in *Uranus* (A92-18701 05-91). Tucson, AZ, University of Arizona Press,  
972 p. 410-465
- 973 Esposito, L. W. & J. E. Colwell (1989), Creation of the Uranus rings and dust  
974 bands, *Nature*, 339, 605-607, doi:10.1038/339605a0.
- 975 European Space Agency (2021), Voyage 2050: Final Recommendations from the Voyage  
976 2050 Senior Committee,  
977 <https://www.cosmos.esa.int/documents/1866264/1866292/Voyage2050-Senior-Committee-report-public.pdf>.
- 979 European Space Agency (2019), Ice Giants: A Mission to the Ice Giants - Neptune  
980 and Uranus, CDF Study Report CDF-187(C), pp. 431.
- 981 Fletcher, L. N., et al. (2020a), Ice Giant Systems: The Scientific Potential of  
982 Orbital Missions to Uranus and Neptune, *Planet Space Sci*, 191, 105030  
983 doi:10.1016/j.pss.2020.105030.
- 984 Fletcher, Leigh N., Imke de Pater, Glenn S. Orton, Mark D. Hofstadter, Patrick  
985 G. J. Irwin, Michael Roman, Daniel Toledo (2020b), *Ice Giant Circulation  
986 Patterns: Implications for Atmospheric Probes*, *Space Science Reviews*, 216, 21  
987 <https://dx.doi.org/10.1007/s11214-020-00646-1>.
- 988 Fletcher, L. N. et al. (2020c), Ice giant system exploration in the 2020s: an  
989 introduction, *Phil. Trans. R. Soc. A.*, 378, doi:10.1098/rsta.2019.0473.
- 990 Fortney, J., Marley, M., Mayorga, L., & Rymer, A. (2021). Synergy between Ice  
991 Giant and Exoplanet Exploration: The Solar System's Planets "As  
992 Exoplanets." *Bulletin of the AAS*, 53(4).  
993 <https://doi.org/10.3847/25c2cfb.7091f439>
- 994 French, R. G. et al. (1991). Dynamics and structure of the Uranian rings. in  
995 *Uranus* (A92-18701 05-91). Tucson, AZ, University of Arizona Press, p. 327-  
996 409.
- 997 French, R. G., et al. (2015), Resonances, Chaos, and Short-term Interactions  
998 Among the Inner Uranian Satellites, *Astron. J.*, 149, 142, doi:10.1088/0004-  
999 6256/149/4/142.
- 1000 French, R. G., et al. (1988), Uranian Ring Orbits from Earth-Based and Voyager  
1001 Occultation Observations, *Icarus*, 73, 349-378, doi:10.1016/0019-  
1002 1035(88)90104-2.
- 1003 French, R. S. & M. R. Showalter (2012), Cupid is doomed: An analysis of the  
1004 stability of the inner uranian satellites, *Icarus*, 220, 911-921,  
1005 doi:10.1016/j.icarus.2012.06.031.

- 1006 Friedson, A. J. & E. J. Gonzales (2017), Inhibition of ordinary and diffusive  
1007 convection in the water condensation zone of the ice giants and implications  
1008 for their thermal evolution, *Icarus*, 297, 160-178,  
1009 doi:10.1016/j.icarus.2017.06.029.
- 1010 Gierasch, P. J. & B. J. Conrath (1987), Vertical temperature gradients on  
1011 Uranus: Implications for layered convection, *J. Geophys. Res. Space Phys.*,  
1012 92(A13), 15019-15029, doi:10.1029/JA092iA13p15019.
- 1013 Girija et al. (2020), Feasibility and Mass-Benefit Analysis of Aerocapture for  
1014 Missions to Venus, *J. Spacecraft Rockets*, 57, doi:10.2514/1.A34529.
- 1015 Greenberg, R. et al. (1991), Miranda, in *Uranus*, Tucson, AZ: University of  
1016 Arizona Press, pp. 693-735.
- 1017 Grundy, W. M. et al. (2016), Surface compositions across Pluto and Charon,  
1018 *Science*, 351, aad9189, doi:10.1126/science.aad9189
- 1019 Grundy et al. (2020). Color, composition, and thermal environment of Kuiper  
1020 Belt object (486958) Arrokoth}, *Science*, 367, 6481,  
1021 doi:10.1126/science.aay3705.
- 1022 Grundy, W. M., et al. (2006), Distributions of H<sub>2</sub>O and CO<sub>2</sub> ices on Ariel,  
1023 Umbriel, Titania, and Oberon from IRTF/Spex observations, *Icarus*, 184, 543-  
1024 555, doi:10.1016/j.icarus.2006.04.016.
- 1025 Guillot, T. Uranus and Neptune are key to understand planets with hydrogen  
1026 atmospheres. *Exp Astron* (2021). <https://doi.org/10.1007/s10686-021-09812-x>
- 1027 Hall, J. L., et al. (2005), Cost-Benefit Analysis of the Aerocapture Mission  
1028 Set, *J. Spacecraft Rockets*, 42, 2, 309-320, doi:10.2514/1.4118.
- 1029 Hammel, H.B., et al. (2009), The Dark Spot in the atmosphere of Uranus in 2006:  
1030 Discovery, description, and dynamical simulations, *Icarus*, 201, 257-271,  
1031 doi:10.1016/j.icarus.2008.08.019.
- 1032 Hapke, B. (2012). Theory of Reflectance and Emittance Spectroscopy, 2nd edn.  
1033 (Cambridge University Press, Cambridge.
- 1034 Hawkins, S.E., Boldt, J.D., Darlington, E.H. et al. The Mercury Dual Imaging  
1035 System on the MESSENGER Spacecraft. *Space Sci Rev* 131, 247-338 (2007).  
1036 doi:10.1007/s11214-007-9266-3.
- 1037 Hedman, M. & Chancia, R. (2021), Uranus's Hidden Narrow Rings. *Planet. Sci. J.*  
1038 2, 107. doi: 10.3847/PSJ/abfdb6.
- 1039 Helled, R. & P. Bodenheimer (2014), The formation of Uranus and Neptune:  
1040 Challenges and implications for intermediate-mass exoplanets, *ApJ*, 789(1),  
1041 69, doi:10.1088/0004-637X/789/1/69.

- 1042 Helled, R., Nettelmann, N. & Guillot, T. Uranus and Neptune: Origin, Evolution  
1043 and Internal Structure. *Space Sci Rev*, 216, 38 (2020).  
1044 <https://doi.org/10.1007/s11214-020-00660-3>.
- 1045 Helled, Ravit and Jonathan Fortney (2020). The interiors of Uranus and Neptune:  
1046 current understanding and open questions. *Phil. Trans. R. Soc. A.*, 378,  
1047 doi:10.1098/rsta.2019.0474.
- 1048 Helled, R. and Guillot, T., (2017). Internal structure of giant and icy planets:  
1049 importance of heavy elements and mixing, in *Handbook of Exoplanets* (eds. H.  
1050 Deeg & J. Belmonte), pp.1-19, Springer, doi:10.1007/978-3-319-30648-3\_44-1.
- 1051 Helled, R., et al. (2011), Interior models of Uranus and Neptune, *ApJ*, 726(1),  
1052 15, doi:10.1088/0004-637X/726/1/15.
- 1053 Hendrix, A. R. et al. (2019), The NASA Roadmap to Ocean Worlds, *Astrobiology*,  
1054 19, 1, doi:10.1089/asr.2018.1955.
- 1055 Hendrix, A., et al., (2012), Mimas' far-UV albedo: Spatial variations, *Icarus*,  
1056 <http://dx.doi.org/10.1016/j.icarus.2012.06.012>
- 1057 Herbert F. (2009), Aurora and magnetic field of Uranus. *J. Geophys. Res. Space  
1058 Phys.* 114, A11206, doi:10.1029/2009JA014394.
- 1059 Herbert, F. & B. R. Sandel (1998), Ultraviolet observations of Uranus and  
1060 Neptune, *Planet. Space Sci.*, 47, 8-9, 1119-1139, doi:10.1016/S0032-  
1061 0633(98)00142-1.
- 1062 Herbert, F. et al (1987), The upper atmosphere of Uranus: EUV occultations  
1063 observed by Voyager 2, *J. Geophys. Res.*, 92, 15,093-15, 109,  
1064 doi:10.1029/JA092iA13p15093.
- 1065 Hesselbrock, A. J. & D. A. Minton (2019), Three Dynamical Evolution Regimes for  
1066 Coupled Ring-satellite Systems and Implications for the Formation of the  
1067 Uranian Satellite Miranda, *Astron. J.*, 157, 30, doi:10.3847/1538-3881/aaf23a.
- 1068 Hibbitts, C. A., K. Stockstill-Cahill, B. Wing, and C. Paranicas (2019). Color  
1069 centers in salts - Evidence for the presence of sulfates on Europa. *Icarus*,  
1070 326, 37-47, doi:10.1016/j.icarus.2019.02.022
- 1071 Hofstadter, M. et al. (2019), Uranus and Neptune missions: A study in advance  
1072 of the next Planetary Science Decadal Survey, *Planet. Space Science*, 177,  
1073 104680, doi:10.1016/j.pss.2019.06.004.
- 1074 Hofstadter, M. et al. (2017), Ice Giants Pre-Decadal Survey Mission Study  
1075 Report, JPL D-100520, pp. 529.
- 1076 Holme, R. & J. Bloxham (1996), The magnetic fields of Uranus and Neptune:  
1077 Methods and models, *J. Geophys. Res.*, 101, E1, 2177-2200,  
1078 doi:10.1029/95JE03437.

- 1079 Howett, C. J. A. et al. (2021). Persephone: A Pluto-system Orbiter and Kuiper  
1080 Belt Explorer. *Planet. Sci. J.*, 2, 75. doi:10.3847/PSJ/abe6aa.
- 1081 Howett, C. J. A., J. R. Spencer, and T. A. Nordheim (2020). Bolometric bond  
1082 albedo and thermal inertia maps of Mimas. *Icarus*, 348:113745, doi:  
1083 10.1016/j.icarus.2020.113745.
- 1084 Hsu, H.-W., Sulaiman, A., Cao, H., Hedman, M. M., Agiwal, O., Altobelli, N., ...  
1085 Jr., J. H. W. (2021). Ice Giants – The Return of the Rings. *Bulletin of the*  
1086 *AAS*, 53(4). <https://doi.org/10.3847/25c2cfab.b28bf609>
- 1087 Hubbard, W. B. (2010), Ice Giants Decadal Study, NASA Mission Concept Study  
1088 Final Report submitted to 2011 Decadal Survey, pp. 290.
- 1089 Hueso, R., T. Guillot, A. and Sánchez-Lavega A. (2020). Convective storms and  
1090 atmospheric vertical structure in Uranus and Neptune. *Phil. Trans. R. Soc. A*,  
1091 378, doi:10.1098/rsta.2019.0476.
- 1092 Hussmann, H., et al. (2002), Thermal equilibrium states of Europa's ice shell:  
1093 Implications for internal ocean thickness and surface heat flow, *Icarus*, 156,  
1094 143–151, doi:10.1006/icar.2001.6776.
- 1095 Ingersoll, A.P. (1999). Atmospheres of the giant planets, in *The New Solar*  
1096 *System*, fourth edition, edited by J. K. Beatty, C. C. Petersen, and A. Chaikin,  
1097 Sky Publishing Corp., Cambridge, Mass. and Cambridge University Press, pp.  
1098 201–220.
- 1099 Irwin, P.G.J., Toledo, D., Garland, R. et al. (2018). Detection of hydrogen  
1100 sulfide above the clouds in Uranus's atmosphere. *Nat Astron* 2, 420–427.  
1101 <https://doi.org/10.1038/s41550-018-0432-1>
- 1102 Janes, D. M., and Melosh, H. J. (1988), Sinker tectonics: An approach to the  
1103 surface of Miranda, *J. Geophys. Res.*, 93(B4), 3127–3143,  
1104 doi:10.1029/JB093iB04p03127.
- 1105 Jankowski, D. G. and S. W. Squyres (1988), Solid-State Ice Volcanism on the  
1106 Satellites of Uranus, 241, 4871, 1322–1325,  
1107 doi:10.1126/science.241.4871.1322.
- 1108 Jarmak, S. et al. (2020). QUEST: A New Frontiers Uranus orbiter mission concept  
1109 study. *Acta Astr.*, 170, 6–26, doi:10.1016/j.actaastro.2020.01.030.
- 1110 Johnson, T. V., Brown, R. H., and Pollack, J. B. (1987), Uranus satellites:  
1111 Densities and composition, *J. Geophys. Res.*, 92(A13), 14884–14894,  
1112 doi:10.1029/JA092iA13p14884.
- 1113 Johnson, T.V., Yeates, C.M. & Young, R. Space science reviews volume on Galileo  
1114 Mission overview. *Space Sci Rev* 60, 3–21 (1992).  
1115 <https://doi.org/10.1007/BF00216848>

- 1116 Juhász, A. and M. Horányi (2002), Saturn's E ring: A dynamical approach, *J.*  
1117 *Geophys. Res.* 107, 1.
- 1118 Karkoschka, E. (2015), Uranus' southern circulation revealed by Voyager 2:  
1119 Unique characteristics. *Icarus*, 250, 294-307,  
1120 doi:10.1016/j.icarus.2014.12.003.
- 1121 Karkoscka, E. (2001). Comprehensive Photometry of the Rings and 16 Satellites  
1122 of Uranus with the Hubble Space Telescope. *Icarus*, 151, 1, 51-68,  
1123 doi:10.1006/icar.2001.6596.
- 1124 Kasper, J.C., Abiad, R., Austin, G. et al. Solar Wind Electrons Alphas and  
1125 Protons (SWEAP) Investigation: Design of the Solar Wind and Coronal Plasma  
1126 Instrument Suite for Solar Probe Plus. *Space Sci Rev*, 204, 131-186 (2016).  
1127 <https://doi.org/10.1007/s11214-015-0206-3>.
- 1128 Kaspi, Y., Showman, A., Hubbard, W. et al. (2013). Atmospheric confinement of  
1129 jet streams on Uranus and Neptune. *Nature*, 497, 344-347,  
1130 doi:10.1038/nature12131.
- 1131 Kinnison, J. et al., "Interstellar Probe: A Practical Mission to Escape the  
1132 Heliosphere," 2021 *IEEE Aerospace Conference (50100)*, 2021, pp. 1-16, doi:  
1133 10.1109/AERO50100.2021.9438249.
- 1134 Krimigis, S. M. et al. (1986). The Magnetosphere of Uranus: Hot Plasma and  
1135 Radiation Environment. *Science*, 233, 4759, doi:10.1126/science.233.4759.97.
- 1136 Kurosaki, K. and M. Ikoma (2017). Acceleration of Cooling of Ice Giants by  
1137 Condensation in Early Atmospheres. *Astrophys. J.*, 153, 260, doi:10.3847/1538-  
1138 3881/aa6faf.
- 1139 Kurth, W. S., and Gurnett, D. A. (1991), Plasma waves in planetary  
1140 magnetospheres, *J. Geophys. Res.*, 96(S01), 18977-18991,  
1141 doi:10.1029/91JA01819.
- 1142 Lanzerotti, L. J., W. L. Brown, C. G. Maclennan, A. F. Cheng, S. M. Krimigis,  
1143 R. E. Johnson (1987), Effects of charged particles on the surfaces of the  
1144 satellites of Uranus. *J. Geophys. Res.* 92(A13), 14949-14957,  
1145 <https://doi.org/10.1029/JA092iA13p14949>
- 1146 Leconte, J., F. Selsis, F. Hersant, T. Guillot (2021), Condensation-inhibited  
1147 convection in hydrogen-rich atmospheres - Stability against double-diffusive  
1148 processes and thermal profiles for Jupiter, Saturn, Uranus, and Neptune, *A&A*,  
1149 598, A98, <https://doi.org/10.1051/0004-6361/201629140>.
- 1150 Lee, Young and Brian Bairstow (2015). Radioisotope power systems reference book  
1151 for mission designers and planners. NASA Jet Propulsion Laboratory Report for  
1152 NASA Planetary Science Division (JPL 15-6), <http://hdl.handle.net/2014/45467>.

- 1153 Leonard, E. et al. (2021). UMaMI: A New Frontiers-style Mission Concept to  
1154 Explore the Uranian System. *Planet. Sci. J.*, 2, 174, doi:10.3847/PSJ/ac0e3b.
- 1155 Li et al. (2018). Moist Adiabats with Multiple Condensing Species: A New Theory  
1156 with Application to Giant-Planet Atmospheres. *J. Atmos. Sci.*, 1063-1072,  
1157 doi:10.1175/JAS-D-17-0257.1.
- 1158 Li, C. & A. P. Ingersoll (2015), Moist convection in hydrogen atmospheres and  
1159 the frequency of Saturn's giant storms, *Nature Geosci.*, 8, 398-403,  
1160 doi:10.1038/NGEO2405.
- 1161 Masters, A. and K.M. Soderlund, Passive electromagnetic sounding of Uranus'  
1162 interior near equinox?, *J. Geophys. Res. Space Physics*, in revision.
- 1163 Matthes, C. S. R., et al. (2018). "Next-generation radioisotope thermoelectric  
1164 generator study," 2018 IEEE Aerospace Conference, pp. 1-9,  
1165 doi:10.1109/AERO.2018.8396738.
- 1166 Mauk, B. H., Krimigis, S. M., Keath, E. P., Cheng, A. F., Armstrong, T.  
1167 P., Lanzerotti, L. J., Gloeckler, G., and Hamilton, D. C. (1987), The hot  
1168 plasma and radiation environment of the Uranian magnetosphere, *J. Geophys.  
1169 Res.*, 92(A13), 15283- 15308, doi:10.1029/JA092iA13p15283.
- 1170 Mauk, B. H., and N. J. Fox (2010), Electron radiation belts of the solar system,  
1171 *J. Geophys. Res.*, 115, A12220, doi:10.1029/2010JA015660.
- 1172 Mauk, B. H. (2014), Comparative investigation of the energetic ion spectra  
1173 comprising the magnetospheric ring currents of the solar system, *J. Geophys.  
1174 Res. Space Physics*, 119, 9729-9746, doi:10.1002/2014JA020392.
- 1175 McAdams et al. (2011). Conceptual Mission Design of a Polar Uranus Orbiter and  
1176 Satellite Tour. *Adv. Astronaut.Sci.*, 140, 11-188.
- 1177 McComas, D.J., Alexander, N., Allegrini, F. et al. The Jovian Auroral  
1178 Distributions Experiment (JADE) on the Juno Mission to Jupiter. *Space Sci  
1179 Rev* 213, 547-643 (2017). <https://doi.org/10.1007/s11214-013-9990-9>
- 1180 McKinnon, W. B. et al. (2009), Exploration Strategy for the Outer Planets 2013-  
1181 2022: Goals and Priorities, Outer Planets Assessment Group White Paper,  
1182 submitted to the National Academies of Sciences, Engineering and Medicine,  
1183 Space Studies Board, 15 Sep 2009.
- 1184 McKinnon, W. B., et al. (1991), Cratering of the Uranian satellites, in *Uranus*,  
1185 Tucson, AZ: University of Arizona Press, pp. 629-692.
- 1186 McKinnon, W. B., (1988), Odd tectonics of a rebuilt moon, *Nature*, 333, 701-702,  
1187 doi:10.1038/333701a0.
- 1188 McNutt Jr., R.L., R.S. Selesnick, J.D. Richardson, Low-energy plasma  
1189 observations in the magnetosphere of Uranus. *J. Geophys. Res.* 92(A5), 4399-  
1190 4410 (1987). <https://doi.org/10.1029/JA092iA05p04399>

- 1191 Melin, H. (2020). The upper atmospheres of Uranus and Neptune. *Phil. Trans. R.*  
1192 *Soc. A.*, 378, doi:10.1098/rsta.2019.0478.
- 1193 Molter, E. M., et al. (2021). Tropospheric Composition and Circulation of Uranus  
1194 with ALMA and the VLA. *Planet. Sci. J.*, 2, 3, doi: 10.3847/PSJ/abc48a.
- 1195 Moses, J. I., et al. (2020). Atmospheric chemistry on Uranus and Neptune. *Phil.*  
1196 *Trans. R. Soc. A.*, 378, doi:10.1098/rsta.2019.0477.
- 1197 Mousis, O. et al. (2020). The role of ice lines in the formation of Uranus and  
1198 Neptune. *Phil. Trans. R. Soc. A.*, 378, doi:10.1098/rsta.2020.0107.
- 1199 Murray, C. & Thompson, R. (1990), Orbits of shepherd satellites deduced from  
1200 the structure of the rings of Uranus. *Nature* 348, 499-502. doi:  
1201 10.1038/348499a0.
- 1202 National Research Council (2011), Vision and Voyages for Planetary Science in  
1203 the Decade 2013-2022, Washington, DC: The National Academies Press,  
1204 doi:10.17226/13117.
- 1205 National Research Council (2018), Visions into Voyages for Planetary Sciences  
1206 in the Decade 2013-2022: A Midterm Review, Washington, DC: The National  
1207 Academies Press, doi:10.17226/25186.
- 1208 Nettelmann, N., et al. (2016). Uranus evolution models with simple thermal  
1209 boundary layers. *Icarus*, 275, 107-116, doi:10.1016/j.icarus.2016.04.008.
- 1210 Nettelmann, N. et al. (2013). New indication for a dichotomy in the interior  
1211 structure of Uranus and Neptune from the application of modified shape and  
1212 rotation data, *Planet. Space Sci.*, 77, 143-151, doi:10.1016/j.pss.2012.06.019.
- 1213 Nicholson, P. D. et al. (2018). The Rings of Uranus. In *Planetary Ring Systems.*  
1214 *Properties, Structure, and Evolution* (9781316286791; Eds. M.S. Tiscareno &  
1215 C.D. Murray). Cambridge University Press, p. 93-111.Ockert, M. E., et al.  
1216 (1987), Uranian Ring Photometry: Results From Voyager 2, *J. Geophys. Res.*,  
1217 92, 14969-14978, doi:10.1029/JA092iA13p14969.
- 1218 Olsen, N. & M. Mandea (2008), Rapidly changing flows in the Earth's core, *Nature*  
1219 *Geoscience*, 1(6), 390, doi:10.1038/ngeo203.
- 1220 Orton, G., Atkinson, D., Balint, T., Hofstadter, M., Mousis, O., Sayanagi, K.,  
1221 & Spilker, T. (2021). Science Return from In Situ Probes in the Atmospheres  
1222 of the Ice Giants. *Bulletin of the AAS*, 53(4).  
1223 <https://doi.org/10.3847/25c2cfeb.b804c71f>
- 1224 Pappalardo, R. T., et al. (1997), Extensional tilt blocks on Miranda: Evidence  
1225 for an upwelling origin of Arden Corona, *J. Geophys. Res. Planets*, 102 (E6),  
1226 13369-13379, doi:10.1029/97JE00802.
- 1227 Paty, C. et al. (2020). Ice giant magnetospheres. *Phil. Trans. R. Soc. A.*, 378,  
1228 doi:10.1098/rsta.2019.0480.

- 1229 Pearl, J. C. & B. J. Conrath, (1991), The albedo, effective temperature, and  
1230 energy balance of Neptune, as determined from Voyager data, *J. Geophys. Res.*,  
1231 96, 18921-18930, doi:10.1029/91JA01087.
- 1232 Pearl, J. C., et al. (1990), The albedo, effective temperature, and energy  
1233 balance of Uranus, as determined from Voyager IRIS data, *Icarus*, 84, 12-28,  
1234 doi:10.1016/0019-1035(90)90155-3.
- 1235 Peterson, G., et al. (2015), Elastic thickness and heat flux estimates for the  
1236 uranian satellite Ariel, *Icarus*, 250, 116-122, 10.1016/j.icarus.2014.11.007.
- 1237 Pirraglia, J. A. (1984), Meridional energy balance of Jupiter, *Icarus*, 59(2),  
1238 169-176, doi:10.1016/0019-1035(84)90020-4.
- 1239 Piszczor, M. F., et al. (2008). Advanced solar cell and array technology for  
1240 NASA deep space missions. *2008 33rd IEEE Photovoltaic Specialists Conference*,  
1241 1-5, doi:10.1109/PVSC.2008.4922856.
- 1242 Podolak et al. (2019). Effect of non-adiabatic thermal profiles on the inferred  
1243 compositions of Uranus and Neptune. *Mon. Not. R. Astron. Soc.*, 487, 2, 2653-  
1244 2664, <https://doi.org/10.1093/mnras/stz1467>
- 1245 Porco, C. C., et al. (2006), Cassini Observes the Active South Pole of Enceladus,  
1246 *Science*, 311, 5766, 1393-1401, doi:10.1126/science.1123013.
- 1247 Porco, C. C. & P. Goldreich (1987), Shepherding of the Uranian Rings. I.  
1248 Kinematics, *Astron. J.*, 93, 3, doi:10.1086/114354.
- 1249 Qualls, A. L., P. Schmitz, J. Rusick, J. F. Zakrajsek, D. F. Woerner and D.  
1250 Cairns-Gallimore, "Dynamic Radioisotope Power System development for space  
1251 exploration," *2017 IEEE Aerospace Conference*, 2017, pp. 1-7,  
1252 doi:10.1109/AERO.2017.7943892.
- 1253 Raut, U. et al. (2008). Cosmic Ray Compaction of Porous Interstellar Ices.  
1254 *Astrophys. J.*, 687(2), 1070-1074, doi: 10.1086/592193.
- 1255 Raynaud, E. et al. (2003), The 10 October 1999 HIP 9369 occultation by the  
1256 northern polar region of Jupiter: ingress and egress lightcurves analysis,  
1257 *Icarus*, 162(2), 344-361, doi:10.1016/S0019-1035(03)00005-8.
- 1258 Roman, M. T. et al. (2020). Uranus in Northern Midspring: Persistent Atmospheric  
1259 Temperatures and Circulations Inferred from Thermal Imaging. *Astrophys. J.*,  
1260 159, 45. doi: 10.3847/1538-3881/ab5dc7.
- 1261 Ruiz, J. (2005), The heat flow of Europa, *Icarus*, 177(2), 438-446,  
1262 doi:10.1016/j.icarus.2005.03.021.
- 1263 Rymer, A. et al. (2018), Solar System Ice Giants: Exoplanets in our Backyard,  
1264 Exoplanet Science Strategy White Paper, submitted to the National Academies  
1265 of Sciences, Engineering and Medicine, Space Studies Board, 9 Mar 2018,  
1266 arXiv:1804.03573.

- 1267 Rymer, A. M. et al. (2021). Neptune Odyssey: A Flagship Concept for the  
1268 Exploration of the Neptune-Triton System. *Planet. Sci. J.*, 2, 184,  
1269 doi:10.3847/PSJ/abf654.
- 1270 Salyk, C. et al. (2006), Interaction between eddies and mean flow in Jupiter's  
1271 atmosphere: Analysis of Cassini imaging data, *Icarus*, 185, 2, 430-442,  
1272 doi:10.1016/j.icarus.2006.08.007.
- 1273 Sayanagi, K.M., Dillman, R.A., Atkinson, D.H. et al. (2020) Small Next-  
1274 Generation Atmospheric Probe (SNAP) Concept to Enable Future Multi-Probe  
1275 Missions: A Case Study for Uranus. *Space Sci Rev*, 216, 72, doi:10.1007/s11214-  
1276 020-00686-7.
- 1277 Scheibe, L., Nettelmann, N., & Redmer, R. (2019). Thermal evolution of Uranus  
1278 and Neptune-I. Adiabatic models. *Astronomy & Astrophysics*, 632, A70.
- 1279 Schenk, P. M. & Moore, J. M. (2020). Topography and geology of Uranian mid-  
1280 sized icy satellites in comparison with Saturnian and Plutonian satellites.  
1281 *Phil. Trans. R. Soc. A.*, 378, doi:10.1098/rsta.2020.0102.
- 1282 Schenk, P. M. (1991), Fluid volcanism on Miranda and Ariel: Flow morphology and  
1283 composition, *J. Geophys. Res. Solid Earth*, 96(B2), 1887-1906,  
1284 doi:10.1029/90JB01604.
- 1285 Selesnick, R. S. & J. D. Richardson (1986), Plasmasphere formation in  
1286 arbitrarily oriented magnetospheres, *Geophys. Res. Lett.*, 13, 7, 624-627,  
1287 doi:10.1029/GL013i007p00624.
- 1288 Showalter, M. R. (2020). The rings and small moons of Uranus and Neptune. *Phil.*  
1289 *Trans. R. Soc. A.*, 378, doi:10.1098/rsta.2019.0482.
- 1290 Showalter, M. R. & J. J. Lissauer (2006), The Second Ring-Moon System of Uranus:  
1291 Discovery and Dynamics, *Science*, 311, 973-977, doi:10.1126/science.1122882.
- 1292 Smith, B. A., et al (1986), Voyager 2 in the Uranian System: Imaging Science  
1293 Results, *Science*, 233, 43-64, doi:10.1126/science.233.4759.43.
- 1294 Smith, G. R. & D. M. Hunten (1990), Study of planetary atmospheres by absorptive  
1295 occultations, *Rev. Geophys.*, 28, 117-143, doi:10.1029/RG028i002p00117.
- 1296 Soderlund, K. M. and Stanley S. (2020). The underexplored frontier of ice giant  
1297 dynamos. *Phil. Trans. R. Soc. A.*, 378, doi:10.1098/rsta.2019.0479.
- 1298 Soderlund, K. M. et al. (2013), Turbulent models of ice giant internal dynamics:  
1299 Dynamos, heat transfer, and zonal flows, *Icarus*, 224(1), 97-113,  
1300 doi:10.1016/j.icarus.2013.02.014.
- 1301 Soffen, G. A. (1976). Scientific Results of the Viking Missions. *Science*, 194,  
1302 4271, 1274-1276, doi: 10.1126/science.194.4271.1274.
- 1303 Solomon, S. et al., editors. (2019). *Mercury: The View after MESSENGER*.  
1304 Cambridge University Press. pp. 596. ISBN: 9781107154452.

- 1305 Sori, M. M., Bapst, J., Bramson, A. M., Byrne, S., & Landis, M. E. (2017). A  
1306 Wunda-full world? Carbon dioxide ice deposits on Umbriel and other Uranian  
1307 moons. *Icarus*, 290, 1-13.
- 1308 Soyuer, D., Soubiran, F., and Helled, R. (2020). Constraining the depth of the  
1309 winds on Uranus and Neptune via Ohmic dissipation. *Monthly Notices of the*  
1310 *Royal Astronomical Society*, 498(1), 621-638.
- 1311 Soyuer, D., & Helled, R. (2021). Linking Uranus' temperature profile to wind-  
1312 induced magnetic fields. *Monthly Notices of the Royal Astronomical Society*,  
1313 507(1), 1485-1490.
- 1314 Spilker, L. (2019). Cassini-Huygens' exploration of the Saturn system: 13 years  
1315 of discovery. *Science*, 364, 6445, 1046-1051, doi: 10.1126/science.aat3760.
- 1316 Spilker, T. R. (2020). Enabling technologies for ice giant exploration, *Phil.*  
1317 *Trans. R. Soc. A.*, 378, doi:10.1098/rsta.2019.0488.
- 1318 Spilker, T. R. et al. (2018), Qualitative Assessment of Aerocapture and  
1319 Applications to Future Missions, *J. of Spacecraft and Rockets*, 56, 2, 536-  
1320 545, doi:10.2514/1.A34056.
- 1321 Spilker, T. R. et al. (2016), An Assessment of Aerocapture and Applications to  
1322 Future Missions, NASA Jet Propulsion Laboratory Report for NASA Planetary  
1323 Science Division (JPL D-97058).
- 1324 Sromovsky, L. A. et al. (2019), The methane distribution and polar brightening  
1325 on Uranus based on HST/STIS, Keck/NIRC2, and IRTF/SpeX observations through  
1326 2015, *Icarus*, 317, 266-306, doi: 10.1016/j.icarus.2018.06.026.
- 1327 Sromovsky, L. A. et al. (2015), High S/N Keck and Gemini AO imaging of Uranus  
1328 during 2012-2014: New cloud patterns, increasing activity, and improved wind  
1329 measurements, *Icarus*, 258, 192-223, doi:10.1016/j.icarus.2015.05.029.
- 1330 Sromovsky, L. A. et al. (2014), Methane depletion in both polar regions of  
1331 Uranus inferred from HST/STIS and Keck/NIRC2 observations, *Icarus*, 238, 137-  
1332 155, doi:10.1016/j.icarus.2014.05.016.
- 1333 Stanley, S. & J. Bloxham (2004), Convective-region geometry as the cause of  
1334 Uranus' and Neptune's unusual magnetic fields, *Nature*, 428(6979), 151,  
1335 doi:10.1038/nature02376.
- 1336 Stanley, S. & J. Bloxham (2006), Numerical dynamo models of Uranus' and  
1337 Neptune's magnetic fields, *Icarus*, 184(2), 556-572,  
1338 doi:10.1016/j.icarus.2006.05.005.
- 1339 Stephan, K., R. Jaumann, R. Wagner, R. N. Clark, D. P. Cruikshank, C. A.  
1340 Hibbitts, T. Roatsch, H. Hoffmann, R. H. Brown, G. Filacchione, B. J. Buratti,  
1341 G. B. Hansen, T. B. McCord, P. D. Nicholson, and K. H. Baines (2010). Dione's

- 1342 spectral and geological properties. *Icarus*, 206(2):631{652, doi:  
1343 10.1016/j.icarus.2009.07.036.
- 1344 Stern, S.A. The New Horizons Pluto Kuiper Belt Mission: An Overview with  
1345 Historical Context. *Space Sci Rev*, 140, 3-21 (2008).  
1346 <https://doi.org/10.1007/s11214-007-9295-y>.
- 1347 Stern, S.A., Slater, D.C., Scherr, J. et al. ALICE: The Ultraviolet Imaging  
1348 Spectrograph Aboard the New Horizons Pluto-Kuiper Belt Mission. *Space Sci  
1349 Rev.*, 140, 155 (2008). <https://doi.org/10.1007/s11214-008-9407-3>.
- 1350 Stevens, M. H. et al. (1993), An Analysis of the Voyager 2 Ultraviolet  
1351 Spectrometer Occultation Data at Uranus: Inferring Heat Sources and Model  
1352 Atmospheres, *Icarus*, 101, 1, 45-63, doi:10.1006/icar.1993.1005.
- 1353 Stone, E. C. & E. D. Miner (1986), The Voyager 2 Encounter with the Uranian  
1354 System, *Science*, 233, 4759, 39-43, doi:10.1126/science.233.4759.39.
- 1355 Stryke, T. & P. J. Stooke (2008), Umbriel, Oberon, and Titania exhibit large  
1356 canyons, similar to those seen on icy satellites elsewhere, presented at 2008  
1357 LPSC abstract #1362.
- 1358 Teanby N. A., Irwin P. G. J., Moses J. I. and Helled R. (2020). Neptune and  
1359 Uranus: ice or rock giants? *Phil. Trans. R. Soc. A.*, 378,  
1360 doi:10.1098/rsta.2019.0489.
- 1361 Tiscareno, M.S., J.A. Burns, M.H. Hedman and C.C. Porco (2008). "The Population  
1362 of Propellers in Saturn's A Ring." *Astronomical Journal*, 135, 1083-1091.
- 1363 Thorne, R. M., et al. (2013), Rapid local acceleration of relativistic  
1364 radiation-belt electrons by magnetospheric chorus, *Nature*, 504, 411-414,  
1365 doi:10.1038/nature12889.
- 1366 Tripathi, A.K., R.P. Singhal (2008). Whistler-mode instability in  
1367 magnetospheres of Uranus and Neptune. *Planet. Space Sci.* 56, 310-319.
- 1368 Tsang, Y. K., & Jones, C. A. (2020). Characterising Jupiter's dynamo radius  
1369 using its magnetic energy spectrum. *Earth Planet. Sci. Lett.*, 530, 115879,  
1370 <https://doi.org/10.1016/j.epsl.2019.115879>.
- 1371 Tyler, G.L., Linscott, I.R., Bird, M.K. et al. The New Horizons Radio Science  
1372 Experiment (REX). *Space Sci Rev*, 140, 217-259 (2008).  
1373 <https://doi.org/10.1007/s11214-007-9302-3>.
- 1374 Vasyliūnas, V. M. (1986), The convection-dominated magnetosphere of Uranus,  
1375 *Geophys. Res. Lett.*, 13, 7, 621-623, doi:10.1029/GL013i007p00621.
- 1376 Vazan, A., & Helled, R. (2020). Explaining the low luminosity of Uranus: a self-  
1377 consistent thermal and structural evolution. *Astronomy & Astrophysics*, 633,  
1378 A50.

1379 Waite, J. H. et al. (1997), Equatorial X-ray emissions: Implications for  
1380 Jupiter's high exospheric temperatures, *Science*, 276, 104-108,  
1381 doi:10.1126/science.276.5309.104.

1382 Wakeford H. R. and Dalba P. A. (2020). The exoplanet perspective on future ice  
1383 giant exploration. *Phil. Trans. R. Soc. A.*, 378, doi:10.1098/rsta.2020.0054.

1384 Weiss, B. P., Biersteker, J. B., Colicci, V., Goode, A., Castillo-Rogez, J. C.,  
1385 Petropoulos, A. E., & Balint, T. S. (2021). Searching for subsurface oceans  
1386 on the moons of Uranus using magnetic induction. *Geophysical Research Letters*,  
1387 48, e2021GL094758. <https://doi.org/10.1029/2021GL094758>

1388 Zakrajsek, J. (2021). "RPS Program Technology Updates". Presented at Fall 2021  
1389 Outer Planets Assessment Group (OPAG) Meeting - virtual. 30 August 2021.  
1390 <https://www.lpi.usra.edu/opag/meetings/aug2021/presentations/Zakrajsek.pdf>

1391 Zhu, Wei and Subo Dong (2021). Exoplanet Statistics and Theoretical  
1392 Implications, *Annu. Rev. Astron. Astrophys.* 59:291-336

1393

1394 Acknowledgements

1395 Work on this project at APL was funded by internal investment by the APL Civil  
1396 Space Mission Area within the Space Exploration Sector. LNF was supported by a  
1397 European Research Council Consolidator Grant (under the European Union's Horizon  
1398 2020 research and innovation program, grant agreement No 723890) at the  
1399 University of Leicester. Parts of this work were carried out at the Jet  
1400 Propulsion Laboratory, California Institute of Technology, under contract with  
1401 the National Aeronautics and Space Administration. RPS details include pre-  
1402 decisional information - for planning and discussion purposes only.